


Downregulation of Stem-Loop Binding Protein by Nicotine via $\alpha 7$ -Nicotinic Acetylcholine Receptor and Its Role in Nicotine-Induced Cell Transformation

Qi Sun,^{*,†} Danqi Chen,^{*} Amna Raja,^{*} Gabriele Grunig,^{*,‡} Judith Zelikoff,^{*} and Chunyuan Jin ^{*,§,1}

^{*}Department of Environmental Medicine, New York University Grossman School of Medicine, New York, New York 10010, USA; [†]Department of Child and Adolescent Health, School of Public Health, China Medical University, Shenyang, Liaoning 110013, China; [‡]Department of Medicine, New York University Grossman School of Medicine, New York, New York 10010, USA; and [§]Perlmutter Cancer Center, NYU Langone Health, New York, New York 10016, USA

¹To whom correspondence should be addressed at Department of Environmental Medicine, New York University Grossman School of Medicine, 341E 25th Street, New York, NY 10010, USA. E-mail: chunyuan.jin@nyulangone.org

ABSTRACT

The use of electronic-cigarettes (e-cigs) has increased substantially in recent years, particularly among the younger generations. Liquid nicotine is the main component of e-cigs. Previous studies have shown that mice exposed to e-cig aerosols developed lung adenocarcinoma and bladder hyperplasia. These findings implicated a potential role for e-cig aerosols and nicotine in cancer development, although the underlying mechanisms are not fully understood. Here we report that exposure to liquid nicotine or nicotine aerosol generated from e-cig induces downregulation of Stem-loop binding protein (SLBP) and polyadenylation of canonical histone mRNAs in human bronchial epithelial cells and in mice lungs. Canonical histone mRNAs typically do not end in a poly(A) tail and the acquisition of such a tail via depletion of SLBP has been shown to cause chromosome instability. We show that nicotine-induced SLBP depletion is reversed by an inhibitor of $\alpha 7$ -nicotinic acetylcholine receptors ($\alpha 7$ -nAChR) or siRNA specific for $\alpha 7$ -nAChR, indicating a nAChR-dependent reduction of SLBP by nicotine. Moreover, PI3K/AKT pathway is activated by nicotine exposure and CK2 and probably CDK1, 2 kinases well known for their function for SLBP phosphorylation and degradation, are shown to be involved, $\alpha 7$ -nAChR-dependently, in nicotine-induced SLBP depletion. Importantly, nicotine-induced anchorage-independent cell growth is attenuated by inhibition of $\alpha 7$ -nAChR and is rescued by overexpression of SLBP. We propose that the SLBP depletion and polyadenylation of canonical histone mRNAs via activation of $\alpha 7$ -nAChR and a series of downstream signal transduction pathways are critical for nicotine-induced cell transformation and potential carcinogenesis.

Key words: nicotine; e-cigarette; stem-loop binding protein; histone; polyadenylation.

Electronic cigarettes (e-cigs) are battery-operated devices that deliver nicotine in aerosols by electronic heating of a solution usually containing nicotine, solvents propylene glycol (PG) and vegetable glycerin (VG), and flavorings. Nicotine itself has generally been considered noncarcinogenic until recently. As a

consequence, e-cigs are often used as an alternative for conventional cigarettes and thus the use of e-cigs has increased substantially, particularly amongst younger subpopulations ([Bold et al., 2021](#); [Kwon et al., 2021](#)). However, growing numbers of recent studies have recently demonstrated diverse health effects

of e-cigs, including their potential carcinogenicity. For example, mice exposed to e-cig aerosols developed lung adenocarcinoma and bladder urothelial hyperplasia (Lee et al., 2018; Tang et al., 2019). This implicated a potential role for e-cig aerosols and nicotine in lung cancer development. Specifically, genotoxicity was proposed as the cause of nicotine-induced tumorigenesis based on the observation that e-cig aerosols induce mutagenic DNA adducts, ie, cyclic 1, N²- γ -hydroxy-propano-deoxyguanosine [γ -OH-PdG] and O⁶-methylG, and inhibits DNA repair in the lungs of ECS-exposed mice and in human lung epithelial cells (Lee et al., 2018; Tang et al., 2019).

In addition to mutagenic effects, nicotine is believed to exert tumorigenic effects via nicotinic acetylcholine receptors (nAChRs)-mediated activation of a variety of downstream signaling pathways (Grando, 2014; Zhao, 2016). Nicotinic AChRs are expressed in nonneuronal cells, including lung epithelial cells (Cheng et al., 2020). Different nAChR subtypes are overexpressed in various cancers and cancer progression is known to be associated with overexpression of nAChRs (Grando, 2014). Moreover, it has been shown that nAChR genetic variants increase the risk of developing cancer, and that some single-nucleotide polymorphisms in nAChRs regulate the sensitivity to nicotine (Saccone et al., 2010; Zhao, 2016). Major tumorigenic effects of nicotine and principal downstream pathways mediated by nAChRs include facilitated cancer cell growth and proliferation by JAK2/STAT pathway, inhibition of apoptosis by PI3K/AKT pathway, regulation of cancer cell detachment, migration and reattachment by Ca²⁺-dependent recruitment of CAMKII and PKC and subsequent phosphorylation and dephosphorylation of adhesion and cytoskeletal proteins (Paleari et al., 2008; Russo et al., 2006; Xiang et al., 2016). Although numerous signaling pathways are implicated in nicotine-induced toxicity and carcinogenicity, the effector(s) that function at “final” steps in the nAChR-mediated signaling pathways have remained elusive.

Previously we have demonstrated that exposure to arsenic, a heavy metal carcinogen, downregulates the expression of Stem-loop binding protein (SLBP), leading to polyadenylation of canonical histone H3.1 mRNA (Brocato et al., 2014, 2015). The treatment of cells to MG132, a proteasome inhibitor, rescued the arsenic-induced downregulation of SLBP protein, suggesting that proteasomal degradation of SLBP took place in response to extracellular signal(s). In addition, arsenic exposure reduced the SLBP mRNA level which was rescued by inhibitors of histone acetylation and DNA methylation (Brocato et al., 2014), indicating that epigenetic mechanisms were involved in the arsenic-induced transcriptional silencing of the *SLBP* gene.

The result of arsenic-induced polyadenylation of canonical histone H3.1 mRNA was surprising because the expression of replication-dependent canonical histone genes, such as histone H3.1, is largely limited in S phase and their mRNAs do not contain a typical poly(A) tail at their 3' ends like other metazoan genes. Instead, they contain a highly conserved hairpin structure, which is bound by SLBP for proper 3' mRNA processing, generating mature H3.1 mRNA without a poly(A) tail. Mutations of the *SLBP* gene can result in misprocessing of the canonical histone mRNAs, leading to expression of polyadenylated mRNA from each of the canonical histone genes (Lanzotti et al., 2002; Sullivan et al., 2001, 2009). Unlike normally processed canonical histone mRNAs, polyadenylated mRNAs are relatively stable, which results in existence of canonical histone mRNAs outside of the S phase and increase in H3.1 protein level (Brocato et al., 2014; Chen et al., 2020). Polyadenylation of H3.1 mRNA has been shown to lead to displacement of histone variant H3.3 at active

critical gene regulatory regions, causing deregulation of cancer-related genes, cell-cycle arrest, chromosome instability and cell transformation (Chen et al., 2020). These data indicate that overexpression of polyadenylated H3.1 mRNA due to SLBP depletion has potential carcinogenic effects (Brocato et al., 2015; Chen et al., 2020).

In this study, we investigated whether nicotine induces downregulation of SLBP and polyadenylation of canonical histone H3.1 mRNA in normal human bronchial epithelial (NHBE) cells and in mice. Moreover, we characterized the factor(s) and signaling pathway(s) involved in nicotine-induced downregulation of SLBP as well as the role of nAChR activation and SLBP depletion in nicotine-induced cell transformation in cultured human lung epithelial cells.

MATERIALS AND METHODS

Reagents. Nicotine (no. N3876), 2-dimethylamino-4,5,6,7-tetra-bromo-1H-benzimidazole (DMAT, no. SML2044), and Roscovitine (no. R7772) were purchased from Sigma-Aldrich (St Louis, Missouri). Trizol reagent was obtained from Invitrogen (Thermo Fisher Scientific, Waltham, Massachusetts). The enhanced chemiluminescence (ECL) plus kit was purchased from Bio-Rad (Hercules, California). The bicinchoninic acid (BCA) protein assay kit was obtained from Pierce (Thermo Fisher Scientific). The antibodies were purchased as follows: anti-CDK2 (1:1000 dilution, no. ab235941), anti- α 7-nAChR (1:1000 dilution, no. ab216485), anti-histone H3 (1:2000 dilution, no. ab1791), and anti-SLBP (1:2000 dilution, no. ab181972) were from Abcam (Cambridge, Massachusetts); anti-CDK1 (1:1000 dilution, no. 33-1800) and anti-CK2 (1:1000 dilution, no. PA5-95701) were purchased from Invitrogen (Thermo Fisher Scientific); anti-histone H4 (1:500 dilution, no. 05-858), anti-histone 2A (1:500 dilution, no. 07-146), and anti-histone 2B (1:500 dilution, no. 07-371) were from MilliporeSigma (Burlington, Massachusetts); anti-GAPDH (1:2000 dilution, no. sc-47724) was from Santa Cruz Biotechnology (Dallas, Texas). Antibodies against phosphorylated-AKT^{T308} (p-AKT^{T308}, 1:500 dilution, no. 2965), p-AKT^{S473} (1:500 dilution, no. 4060), and AKT (1:1000 dilution, no. 4961s) were from Cell Signaling Technology (Danvers, Massachusetts). All other chemicals were of the analytical grade and obtained from the local chemical suppliers. These chemical reagents were prepared as stock solutions with sterile water (tissue culture grade), and then diluted to the final concentrations before application.

Cell culture and treatment. Immortalized human lung bronchial epithelial BEAS-2B cells were obtained from the American Type Culture Collection (ATCC, Manassas, Virginia) and maintained in DMEM supplemented with 10% FBS, 100 U/ml penicillin, and 100 μ g/ml streptomycin. The primary NHBE cells were purchased from Lonza (Switzerland) and maintained in BEGM medium (Lonza, Switzerland) supplemented with 100 U/ml penicillin and 100 μ g/ml streptomycin. Cells were incubated at 37°C in a humidified atmosphere containing 5% carbon dioxide. In all experiments, cells (0.44×10^6) were seeded into 10 cm-diameter tissue-culture dishes with growth medium and allowed to reach 60% confluence before being exposed to nicotine with doses 0, 500, and 750 μ M for 24 h, or 0, 10, 25, and 50 μ M for 1–4 weeks. For competition inhibition assays, 10 μ M Roscovitine, 0.1 μ M DMAT, 10 or 25 μ M LY294002, 10 μ M Mecamylamine (Sigma-Aldrich, St Louis, Missouri), 10 μ M DH β E or 1 μ M α -bungarotoxin (MilliporeSigma, St Louis, Missouri) was added 1 h before nicotine treatment.

Cell proliferation assay. The 3-(4,5-dimethylthiazol-2-yl)-2,5-diphenyl tetrasodium bromide (MTT, Sigma-Aldrich) cytotoxicity assay measures mitochondrial reductases, which convert the water soluble MTT salt to a formazan that accumulates in healthy cells. A total of 5000/well cells were seeded into 96-well plate, then cells were exposed to increasing concentrations of nicotine after the cells reached 60% confluency. After 24 h of treatment, 10 μ l MTT was added to each well containing 100 μ l fresh medium with final concentration of 5 mg/ml MTT and incubated for 4 h at 37°C in 5% CO₂. At the end of the incubation, 100 μ l of isopropanol containing 0.04 N HCl was added to each well to dissolve the crystals. The absorbance of wells was read at 570 nm using a microplate reader.

Soft-agar assays. Cells treated with or without nicotine were rinsed with PBS then seeded in low-gelling temperature Agarose Type VII (Sigma Aldrich). The cells were seeded in triplicate in 6-well plates (5000 cells/well) in a top layer of 0.35% agarose onto a bottom layer of 0.5% agarose and cultured at 37°C for 6 weeks. Colonies were stained with INT/BCIP (Roche Diagnostics, Indianapolis, Indiana) overnight for visualization and quantification of colony growth in agar and photographed. Colonies larger than 50 μ m were counted. All experiments were performed in triplicates. The results were presented as fold change versus 0 μ M nicotine treatment group after the colonies were adjusted for plating efficiency.

Western blot. Whole cell lysates were prepared from cultured cell using RIPA lysis buffer. For mouse lung tissue lysate, 0.1 g of lung tissue for each sample was shredded and cleaned with pre-cold PBS, followed by sonication in RIPA lysis buffer to get homogenate lysate. Protein concentrations were determined by BCA protein assay (Pierce, Thermo Fisher Scientific). Thirty microgram of whole cell lysate or 80 μ g of tissue lysate per lane were separated by 14% SDS-PAGE and blots were transferred to a polyvinylidene difluoride membrane. The membrane was blocked with 5% skimmed milk in TBST for 30 min at room temperature then incubated with primary antibodies overnight at 4°C and secondary antibody conjugated with horseradish peroxidase for 1 h at room temperature before visualization by ECL Plus Western blotting detection reagent (Bio-Rad, Hercules, California). Semiquantification of the bands were performed using NIH Image J software.

RNA isolation and real-time quantitative PCR. Total RNA was extracted using Trizol Reagent (Invitrogen, Grand Island, New York). Briefly, 1 ml Trizol was directly added to the plate to fully digest the cells followed by phase separation and RNA precipitation. For lung tissues, 0.1 g of tissue for each sample was quickly frozen and ground in liquid nitrogen, then mixed with 1 ml Trizol to extract RNA. The quantity and purity of the RNA prepared from each sample were determined using a NanoDrop 2000 spectrophotometer. Reverse transcription (RT) was performed using SuperScript IV First-Strand Synthesis System (Invitrogen) with 1 μ g of RNA in a final reaction volume of 20 μ l after DNA was removed. After incubation at 50°C for 50 min, RT was terminated by heating at 85°C for 5 min. Quantitative real-time PCR analysis was performed using Power SYBR Green PCR Master Mix (Applied Biosystems, Waltham, Massachusetts). PCR was performed in triplicate. RNA abundance was expressed as 2^{- $\Delta\Delta$ CT} for the target gene normalized against the GAPDH gene and presented as fold change to the level in control cells. The following primers were used:

Gene ID		Primer Sequence
SLBP	Forward	5'-CAAGACACCTTCGACAACCT-3'
	Reverse	5'-GTCCCATGAACGTCGACTATAC-3'
H3.1c	Forward	5'-AAATCGCCAGGACTTCAAA-3'
	Reverse	5'-TCCTGCAGCGCCATCAC-3'
H2Ae1	Forward	5'-GAAAGCAAGCGCGCAAAG-3'
	Reverse	5'-CACACGGCCAACCTGGAAACT-3'
H2Bd1	Forward	5'-CTCAGAAGAAGGACGGGAAGAA-3'
	Reverse	5'-CGGGATGGACCTGCTTCA-3'
H3.2c	Forward	5'-GTCCACGGAGCTGCTGAT-3'
	Reverse	5'-GCAGGTCCGTCTTAAAGTC-3'
H4	Forward	5'-TCCGCGATGCTGTCACCTA-3'
	Reverse	5'-TCCATGGCTGTGACTGTCTTG-3'
GAPDH	Forward	5'-TGCACCACCAACTGCTTAGC-3'
	Reverse	5'-GGCATGGACTGTGGTCATGA-3'

Immunofluorescence staining. After washing twice with PBS, cells were fixed with 10% formaldehyde, and incubated with 5% BSA at room temperature to block nonspecific binding of antiserum. Cells were incubated with primary antibodies against α 7-nAChR (1:150 dilution) at 4°C overnight. Labeled cells were visualized by the use of FITC-conjugated secondary antibodies (goat anti-rabbit) for 1 h at room temperature. A final concentration of 0.1 μ g/ml DAPI was then added for 10 min and digital images were captured using ZOE Fluorescent Cell Imager (Bio-Rad). For negative controls, the primary antibodies were omitted.

Cell transfection and siRNA knockdown. CDK1, CDK2, CK2 α 1, CK2 α 2, and α 7-nAChR siRNAs were purchased from Thermo Fisher (catalog nos. 103821, 118638 146139, 103306, and 114074). Cells were seeded 24 h before transfection in complete medium without antibiotics to allow 60%–80% confluency at transfection. Lipofectamine RNAiMax (Invitrogen, catalog no. 13778150) and siRNAs were each diluted in serum-free medium. The resulting 2 solutions were then mixed and incubated to enable complex formation. Cells were then transfected by adding the RNAi-Lipofectamine complex dropwise to medium to achieve a final siRNA concentration of 80 pmol/l (for CDK1, CDK2, CK2 α 1, and CK2 α 2) and 40 pmol/l (for α 7-nAChR), and cells in negative control group were transfected with universal negative siRNA. Cells were incubated at 37°C and knockdown efficiency was examined at 48 h post-transfection.

pcDNA-FLAG-SLBP plasmids were purified using a commercial Qiagen QIAprep Spin Midiprep kit before transfection. Overexpression transfections were performed using Lipofectamine LTX Reagent with PLUS reagent (Invitrogen) following the manufacturer's protocol. Briefly, 1.5 \times 10⁶ cells were seeded into 6-well dishes 24 h prior to transfection. The following day, purified plasmid (1 μ g) was transfected into cells in each well with 10 μ l of Lipofectamine LTX and 2.5 μ l of PLUS reagent. After 24 h post-transfection, the media was removed and replaced with fresh DMEM. 0.5 μ g/ml of G418 selection agent was added to the transfected cells 3 days later. The cells were grown under selection for 3 weeks and harvested for Western blot and qPCR analysis.

E-cig aerosol exposure. Prior to e-cig aerosols exposure, BEAS-2B cells were detached by 0.05% trypsin solution and seeded into Transwell plates containing 0.4 μ m pore size polyester

membrane inserts in each of 6-well culture plates, at a seeding density of 120 000/insert. NHBE cells were detached by trypsin pre-warmed at 37°C and seeded into the Transwell inserts with at a density of 240 000/insert. Twenty-four hours after seeding, medium on the apical side of the membrane was removed from the insert to create an air-liquid interface, and cells on the membrane were exposed to either filtered clean air (FA) or e-cig aerosols. Unflavored tobacco e-liquid purchased from a U.S. brand (Halo) was used in this study with 50% PG and 50% VG (50:50 PG/VG), containing 0 or 18 mg/ml nicotine. E-cig aerosols were produced from an automated 3-port e-cig aerosol generator (e~Aerosols LLC), as described previously (Lauterstein et al., 2016). Puff aerosols were generated with charcoal and HEPA-FA using a rotor-less diaphragm pump; the puff regimen consisted of 55 ml puff volumes of 3 s duration at 30 s intervals at 3.6 V voltage. Each puff was mixed with filtered dilution air before entering the exposure chamber. After exposure for 20 min, medium on the apical side of the membrane was added and the cells incubated for 24 h in normal culture condition (37°C in a humidified atmosphere containing 5% carbon dioxide).

Animal exposure. For *in vivo* experiments, 8-week-old female A/J mice were randomly divided into 3 exposure groups consisting of FA group, PG/VG (50:50) group, and a nicotine (36 mg/ml) plus PG/VG group. The whole-body inhalation exposure was performed at the University of Rochester. The e-cigarette (EC) machine was designed to vary puff profile parameters, such as operating voltage, flow rate, and puff duration and to accommodate disposable EC and future EC generations, and has been used in a number of published *in vivo* and *in vitro* studies at NYU (Church et al., 2020; Lauterstein et al., 2016; Zelikoff et al., 2018) and other universities. This automated 3-port EC aerosol generator (e~Aerosols, developed in Dr Gordon's lab at NYU Grossman School of Medicine) was used with 3rd generation NJOY EC tanks, a popular and widely used e-cig brand with nicotine. Each day, freshly made e-liquids (50% PG, 50% VG), with or without nicotine (36 mg/ml) were used for EC exposures. Before use, the electrical resistance of each EC was measured to ensure the integrity of the heating coils, and the voltage adjusted to produce a consistent wattage for each EC. The aerosol puffs were generated with charcoal- and HEPA-FA with a regime of 55 ml puff volume of 4 s duration at 30-s intervals for 5 min. To simulate human vaping profiles, this 5 min puffing profile was repeated every 30 min for 4 h. Each puff was mixed with filtered dilution air before entering the exposure chamber. Mice were exposed to each treatment for 4 h per day, 5 days a week, for 3 months. The target exposure was 50 µg/l by filter weight, the flow rate was 100 l/min. Mice were maintained at a temperature of 21°C–23°C and 40%–60% humidity. After the final day of exposure, the animals were transferred to the NYU Langone vivarium and analyzed 3 months later, to determine long-term consequences of e-cig exposure. The mice were sacrificed and lung tissues were immediately collected and frozen in –80°C. All procedures using animals were approved by the New York University School of Medicine Institutional Animal Care and Use Committee.

Statistical analysis. All data were expressed as mean ± standard deviations (SD), significant differences among and between group means were carried out using Software SPSS v22.0 (SPSS Inc., USA). Significant differences between the means were evaluated by analysis of variance test (1-way ANOVA). Post hoc tests, when appropriate, were analyzed using Dunnett's test. Statistical significance was defined as $p < .05$.

RESULTS

Nicotine Exposure Induces Downregulation of SLBP

Previously, we reported that arsenic exposure induces polyadenylation of canonical histone mRNAs through depletion of SLBP, a key factor for pre-mRNA processing of canonical histones (Brocato et al., 2014). Polyadenylation of canonical histone H3.1 mRNA caused aberrant transcription, cell cycle arrest, and chromosome instability in human lung epithelial cells (Chen et al., 2020). To test the hypothesis that nicotine would have a similar impact on SLBP expression, human lung epithelial BEAS-2B cells were treated with nicotine and the SLBP protein level was measured by Western blot analysis.

To determine suitable nicotine concentrations to be used, cell viability MTT assays were performed with BEAS-2B cells treated with either 250, 500, 750, or 1000 µM nicotine for 24 h. The doses were chosen because an acute increase of nicotine up to 100 µM in serum and 1000 µM at the mucosal surface immediately following smoking have been reported (Armitage et al., 1975; Lindell et al., 1993; Russell et al., 1980). Cell viability was 80% or above at concentrations up to 750 µM (Figure 1A). As sub-cytotoxic doses (>80% cell viability) are considered appropriate for generating meaningful outcomes in *in vitro* carcinogenesis studies (Mathijs et al., 2010; van Kesteren et al., 2011), cells were treated with either 500 or 750 µM. Subsequent experiments at lower doses (approximately 50 µM) are being carried out to validate some of the observed effects. The SLBP protein levels were reduced by about 25% and 45% following exposures to 500 and 750 µM nicotine, respectively, as compared with the control (Figure 1B). By contrast, SLBP mRNA level was decreased only by treatment with 750 µM nicotine, but not by 500 µM, albeit with no statistical significance ($p = .08$), indicating that nicotine downregulates SLBP protein levels perhaps through posttranscriptional regulation under these conditions.

Next, we examined if similar results were observed at lower doses of nicotine that are more relevant to the human scenario. In this case, BEAS-2B cells were treated with 0, 10, 25, and 50 µM of nicotine for 1–4 weeks. The SLBP protein levels were decreased by 30% at 3 weeks during exposure in the 50 µM group ($p < .05$) and by 20% at 4 weeks albeit not significantly ($p = .069$) (Figure 1F and Supplementary Figs. 1A, C, and E). The SLBP mRNA levels were decreased following a 4-week treatment with 50 µM of nicotine, as compared with the 0 µM control group ($p < .05$) (Figure 1G and Supplementary Figs. 1B, D, and F). Taking together, we conclude that exposure of the NHBE cells to liquid nicotine can reduce protein and mRNA levels for SLBP.

Nicotine Exposure Induces Polyadenylation of Canonical Histone H3.1 mRNA and Increases H3 Protein Level

As nicotine exposure reduced SLBP protein level, we investigated whether it induces aberrant 3'-end processing of canonical histone H3.1 mRNA. The level of polyadenylated mRNAs can be determined by using real-time quantitative PCR (RT-qPCR) with oligo (dT) primers for RT, which captures mRNAs with poly(A) tail. Figure 1D reveals that exposure of BEAS-2B cells to 750 µM of nicotine for 24 h results in approximately a 1.5-fold increase of polyadenylated H3.1 mRNA, as compared with the control (Figure 1D). Polyadenylation of mRNAs for other canonical histones including, H2A, H2B, H3.2, and H4 were also increased by exposure of cells to 750 µM nicotine for 24 h (Supplementary Figure 2A). Given that nicotine exposure induced polyadenylation of all canonical histone mRNAs, we then examined how these alterations changes protein levels of all 4 core histones. Results of Western blotting showed that the

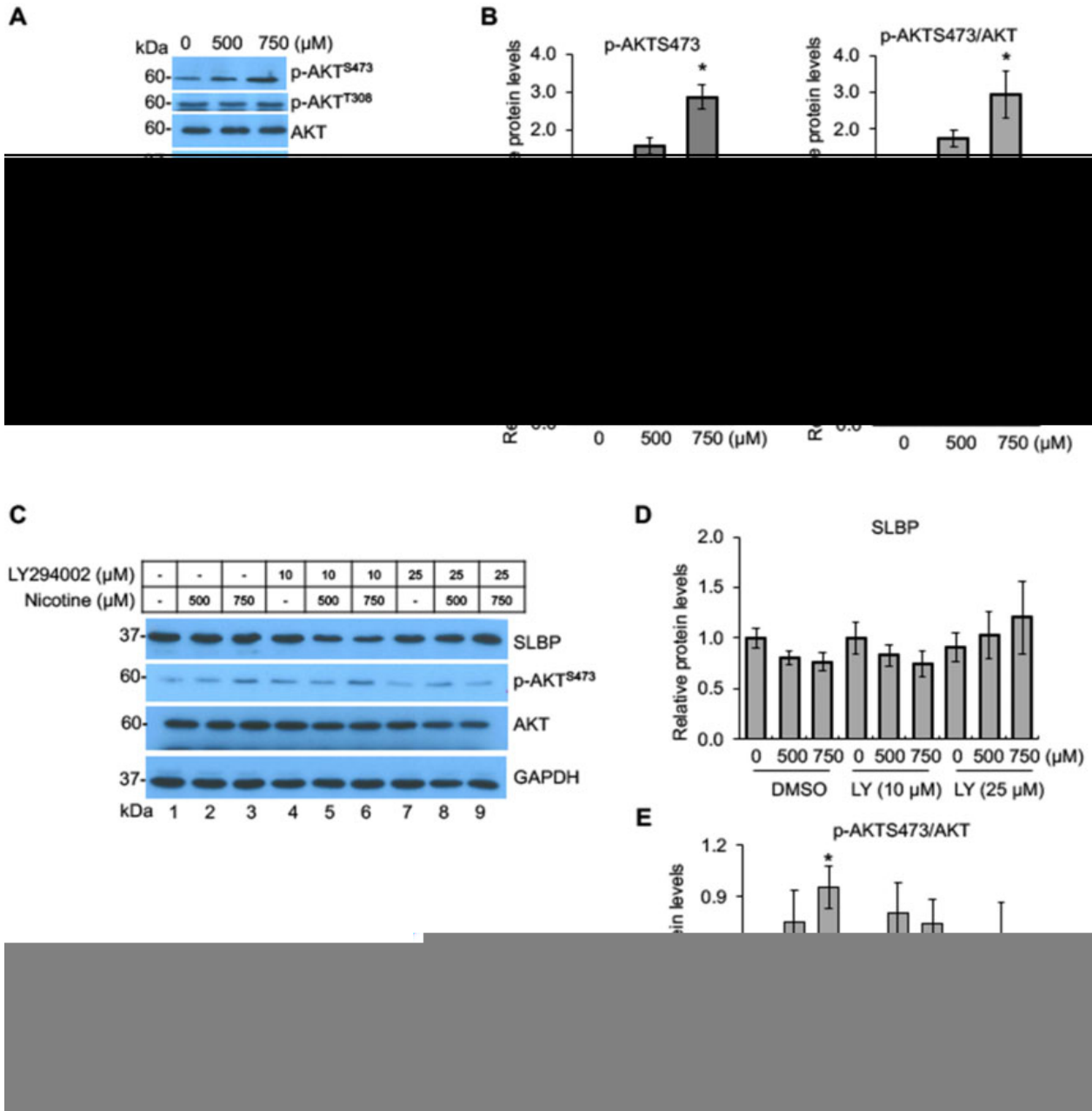


Figure 1. Downregulation of SLBP and polyadenylation of H3.1 mRNA by nicotine. **A**, BEAS-2B cells were treated with various concentrations of nicotine for 24 h and subjected to MTT assays. **B** and **C**, Downregulation of SLBP by nicotine. The SLBP protein level and mRNA level were measured by Western blot (**B**) and RT-qPCR (**C**), respectively, in BEAS-2B cells treated with or without nicotine for 24 h. GAPDH was used as an internal control. The band intensities (left panel in **B**) were quantified using ImageJ software and presented as bar graphs to show relative quantification of SLBP protein level (right panel in **B**). **D** and **E**, Polyadenylation of canonical histone H3.1 mRNA by nicotine. The level of polyadenylated H3.1 mRNA (**F**) and total H3 protein level (**G**) were determined by RT-qPCR and Western blot, respectively, in BEAS-2B cells treated with or without nicotine for 24 h. The amount of polyadenylated H3.1 mRNA was measured by RT-qPCR using cDNAs synthesized with oligo (dT) primers, capturing polyadenylated mRNAs. GAPDH was used as an internal control. The band intensities (left panel in **G**) were quantified and presented as bar graphs (right panel in **G**). **F** and **G**, Downregulation of SLBP by low-dose “long-term” treatment with nicotine. The SLBP protein and mRNA levels were measured by Western blot (**D**) and RT-qPCR (**E**), respectively, in BEAS-2B cells treated with (10, 25, and 50 μM) or without nicotine for 4 weeks. GAPDH was used as an internal control. The band intensities (left panel in **D**) were quantified and presented as bar graphs (right panel in **D**). **H** and **I**, Polyadenylation of canonical histone H3.1 mRNA by low-dose “long-term” treatment with nicotine. The level of polyadenylated H3.1 mRNA (**H**) and total H3 protein level (**I**) were determined by RT-qPCR and Western blot, respectively, in BEAS-2B cells treated with (10, 25, and 50 μM) or without nicotine for 4 weeks. GAPDH was used as an internal control. The band intensities (left panel in **I**) were quantified and presented as bar graphs (right panel in **I**). Untreated controls were used as references, which were set to 1. The data shown are the mean \pm SD ($n = 3$). * $p < .05$ versus untreated control group.

protein levels of total histone H3, as well as H2B and H4 were upregulated following a 24-h treatment with 750 μM nicotine, compared with the untreated control group (Figure 1E and Supplementary Figs. 2B–E).

Next, we determined if polyadenylation of H3.1 mRNA is also induced by low-dose “long-term” treatment of the cells to nicotine. The level of H3.1 mRNA with a poly(A) tail was significantly increased in BEAS-2B cells treated with 50 μM nicotine for

4 weeks, compared with the 0 μ M treatment group (Figure 1H). In contrast, cells treated either with 50 μ M nicotine for 1–3 weeks or with 10 or 25 μ M nicotine for 4 weeks failed to reach statistical significance, compared with the control group (Figure 1H and Supplementary Figs. 3A, C, and E). The H3 protein level was also upregulated by treatment of cells with 50 μ M nicotine for 4 weeks (Figure 1I and Supplementary Figs. 3B, D, and F). These results indicate that *in vitro* exposure to nicotine leads to a loss of SLBP, gain of H3.1 mRNA with poly(A) tail, and an increase in H3 protein.

Nicotine-Mediated SLBP Depletion Is α 7-nAChR Dependent

Nicotine is an agonist of nAChRs (Albuquerque et al., 2009). To gain mechanistic insight into nicotine-induced SLBP depletion, we asked whether the nicotine-induced downregulation of SLBP requires nAChR activation in BEAS-2B cells. nAChRs belong to the superfamily of homologous Cys-loop ion channel receptors, consisting of 9 α (α 2– α 10) and 3 β subunits (β 2– β 4). The upregulation of α 7-nAChR has been shown to be particularly important in lung cancer, facilitating the proliferation and migration of cancer cells in lung tissue (Mucchietto et al., 2016; Schaal and Chellappan, 2014). Immunofluorescence staining of BEAS-2B cells demonstrated a dose-dependent increase of α 7-nAChR protein upon nicotine treatment (Figs. 2A and B). α -BTX, a classical α 7-nAChR inhibitor, completely abrogated nicotine-induced upregulation of α 7-nAChR (Figs. 2A and B). Western blot analysis showed that nicotine-induced reduction of SLBP protein level was attenuated by α 7-nAChR inhibitor α -BTX but not by α 3/ α 4-nAChR inhibitor DH β E (Figs. 2C and D). This finding suggests that the downregulation of SLBP by nicotine is likely dependent specifically on α 7-nAChR.

To further validate an essential role for α 7-nAChR in nicotine-induced SLBP depletion, siRNA was used to knock down α 7-nAChR expression. Immunofluorescence staining revealed a dose-dependent increase of α 7-nAChR protein expression in nicotine-treated BEAS-2B cells that were transfected with the control siRNAs (Figs. 2E and F). In contrast, transfection of siRNA specific for α 7-nAChR abrogated the nicotine-mediated upregulation of α 7-nAChR (Figs. 2E and F). Notably, nicotine-induced depletion of SLBP was attenuated by knockdown of α 7-nAChR expression by siRNA (Figs. 2G and H). Together, we conclude that the nicotine-induced decrease in SLBP is α 7-nAChR dependent.

Activation of PI3K/AKT Signal Transduction Pathway by Nicotine Exposure

It has been reported that the stimulation of nAChRs activates the PI3K/AKT pathway (Kihara et al., 2001). As nicotine upregulated α 7-nAChR, we next investigated if PI3K/AKT pathway is mechanistically involved in the nicotine-induced SLBP depletion. As shown in Figure 3, nicotine treatment significantly increased phosphorylation of AKT at S473 (p-AKT^{S473}), but not p-AKT^{T308}, measured either directly or relative to total AKT (Figs. 3A and B). Total AKT protein levels were not changed by nicotine treatment. To determine whether PI3K/AKT activation was involved in the depletion of SLBP, cells were pretreated with 10 or 25 μ M LY294002, an inhibitor of PI3K, prior to exposure of the cells to nicotine. Nicotine-induced increase in p-AKT^{S473} was reversed by 25 μ M LY294002 and by 10 μ M LY294002 to a lesser extent, indicating that 25 μ M LY294002 efficiently blocked PI3K/AKT pathway (Figs. 3C and E). Western blot analysis further showed that in control cells, the SLBP protein level was decreased by about 20% following nicotine treatment albeit not significantly ($p > .05$) (Figs. 3C and D, lanes 1–3), whereas the

nicotine-induced SLBP reduction was rescued by 25 μ M LY294002 (Figs. 3C and D, lanes 4–9). These results suggest that nicotine activates the PI3K/AKT pathway by inducing phosphorylation of AKT at S473, yet its role in the nicotine-induced downregulation of SLBP was undefined given that no statistical significance for the changes in the SLBP protein level induced by nicotine was observed in the control cells.

Regulation of Nicotine-Induced SLBP Depletion by CDK1/2

The level of SLBP is mainly regulated by posttranscriptional mechanisms in normal cells (Whitfield et al., 2000). Previous studies have demonstrated that phosphorylation of SLBP at Thr61 by cyclin A/CDK1 primes phosphorylation at Thr60 by CK2, which triggers subsequent proteasome-mediated SLBP degradation at the S/G2 cell cycle border (Bradford and Jin, 2021). Thus, we examined if CDK1 and/or CK2 are involved in nicotine-induced SLBP depletion. We first measured the changes of SLBP protein levels following nicotine treatment in the presence of roscovitine, an inhibitor of CDK1, CDK2, CDK5, and CDK7 (Cicenas et al., 2015). Nicotine exposure at 750 μ M reduced the SLBP protein level with statistical significance in the absence of roscovitine (compare lane 1 with lanes 4 in Figs. 4A and B), a similar reduction was not observed in the cells pretreated with roscovitine (compare lane 2 with lanes 6 in Figs. 4A and B), suggesting that CDK1, CDK2, CDK5, and/or CDK7 are required for nicotine-induced SLBP depletion.

For further verifying the role of CDK1/2 in inducing nicotine-induced SLBP downregulation, BEAS-2B cells were transfected with control siRNA or siRNAs specific for either CDK1 or CDK2 followed by the Western blot analysis. The results showed highly efficient knockdown of CDK1 or CDK2 expressions by respective siRNAs (Figs. 4C, D, G, and H). p-AKT^{S473} was upregulated by nicotine exposure in the control cells as seen in the “wild-type” BEAS-2B cells (lanes 1–3 in Figs. 4C, E, G, and I). Interestingly, CDK1 siRNA had no effect on nicotine-induced changes in p-AKT^{S473} (Figs. 4C and E). By contrast, the level of p-AKT^{S473} was greatly inhibited in the CDK2 siRNA cells (Figs. 4G and I), suggesting that CDK2 but not CDK1 was responsible for upregulation of p-AKT^{S473} by nicotine exposure. In the control siRNA cells, nicotine exposure decreased the SLBP protein level by about 30% ($p > .05$), whereas knockdown of either CDK1 or CDK2 was able to reverse nicotine-induced depletion of SLBP (Figs. 4C, F, G, and J). Given that nicotine-induced reduction of SLBP in the control siRNA cells was not statistically significant, further studies are needed to confirm the role of CDK1 and CDK2 in nicotine-mediated SLBP depletion. Nonetheless, they are likely function through different mechanisms that are either p-AKT^{S473}-dependent (CDK2) or independent (CDK1).

SLBP Depletion by Nicotine Is Regulated by CK2

To test if CK2 is also involved in nicotine-mediated SLBP downregulation, we investigated how DMAT, an inhibitor of CK2, affects SLBP protein level following nicotine exposure in BEAS-2B cells. In the absence of DMAT, the SLBP protein level was reduced dose dependently by nicotine treatment (lanes 1–3 in Figs. 5A and B), whereas the SLBP depletion was rescued in the presence of DMAT (lanes 4–6 in Figs. 5A and B). These data suggest a role for CK2 might in the nicotine-induced loss of SLBP.

The role of CK2 in SLBP downregulation was further verified by using siRNAs targeting the α 1 and α 2 catalytic subunit, respectively. Both siRNAs specifically depleted the expression of respective targeting subunits (compare lanes 1 and 4 in Figs. 5C and D and Figs. 5G and H). The protein levels for CK2 α 1 but not CK2 α 2 were significantly upregulated by nicotine treatment in

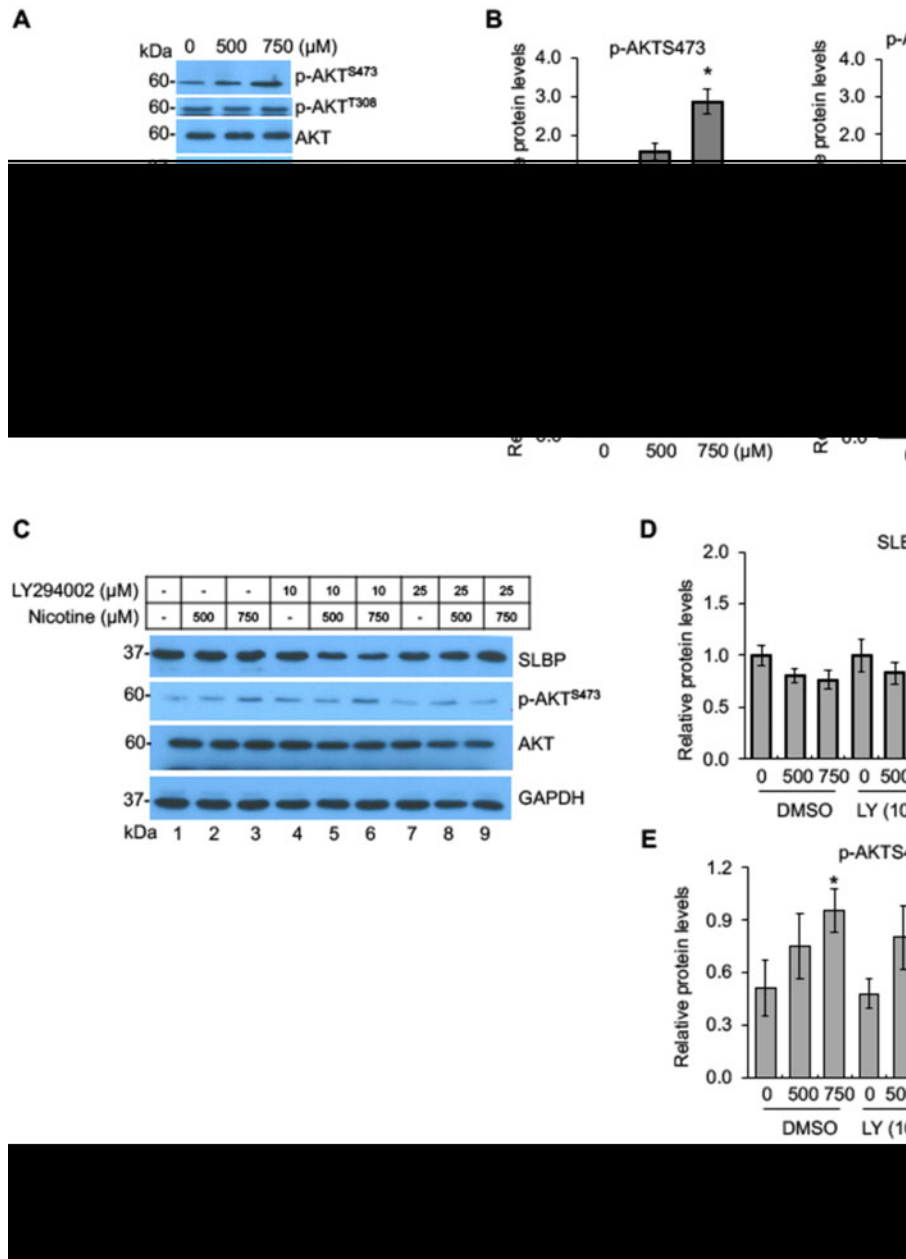


Figure 2. Nicotine-mediated downregulation of SLBP is $\alpha 7$ -nAChR dependent. A–B, Immunofluorescence (IF) staining of $\alpha 7$ -nAChR in BEAS-2B cells treated with or without nicotine for 24 h in the presence or absence of 1 μ M α -BTX, an inhibitor of $\alpha 7$ -nAChR. Representative IF staining for $\alpha 7$ -nAChR, DAPI, and merged images are shown (A). The IF intensities for $\alpha 7$ -nAChR were determined by ImageJ software, normalized to control group, and presented as bar graphs (B). C and D, α -BTX, an inhibitor of $\alpha 7$ -nAChR, but not DH β E, an inhibitor of $\alpha 3/4$ -nAChR, attenuates nicotine-induced downregulation of SLBP. BEAS-2B cells were treated with or without nicotine for 24 h in the presence or absence of DH β E or α -BTX and subjected to Western blot analysis with indicated antibodies (C). The band intensities were quantified and presented as bar graphs to show relative protein levels for SLBP (D). GAPDH was used as an internal control. E–F, IF staining of $\alpha 7$ -nAChR following nicotine treatment of BEAS-2B cells transiently transfected with the control siRNA or the siRNA specific for $\alpha 7$ -nAChR. Representative IF staining for $\alpha 7$ -nAChR (green), DAPI (blue), and merged images are shown (E). The IF intensities for $\alpha 7$ -nAChR were determined by ImageJ software, normalized to control group, and presented as bar graphs (F). G and H, Knockdown of $\alpha 7$ -nAChR by siRNA attenuates nicotine-mediated downregulation of SLBP. BEAS-2B cells that have been transiently transfected with the control siRNA or the siRNA specific for $\alpha 7$ -nAChR were treated with or without nicotine for 24 h and subjected to Western blot analysis with indicated antibodies (G). The band intensities were quantified and presented as bar graphs to show relative protein levels for SLBP (H). GAPDH was used as an internal control. Untreated controls in lane 1 were used as references, which were set to 1. The data shown are the mean \pm SD ($n = 3$). * $p < .05$ versus untreated control group.

the control siRNA cells (lanes 1–3 in Figs. 5C and D and Figs. 5G and H), whereas the induction was not observed in both the CK2 $\alpha 1$ - and CK2 $\alpha 2$ -siRNA cells (lanes 4–6 in Figs. 5C and D and Figs. 5G and H). Notably, the knockdown of CK2 $\alpha 1$ reversed nicotine-induced p-AKT^{S473} and the loss of SLBP (lanes 4–6 in Figs. 5C, E, and F).

By contrast, the CK2 $\alpha 2$ knockdown failed to reverse the depletion of SLBP induced by nicotine exposure (lanes 4–6 in Figs. 5G and J). However, the level of p-AKT^{S473} was not further increased by nicotine treatment in the CK2 $\alpha 2$ siRNA cells probably due to the amount of p-AKT^{S473} has already reached saturation by CK2 $\alpha 2$ knockdown even prior to the nicotine treatment

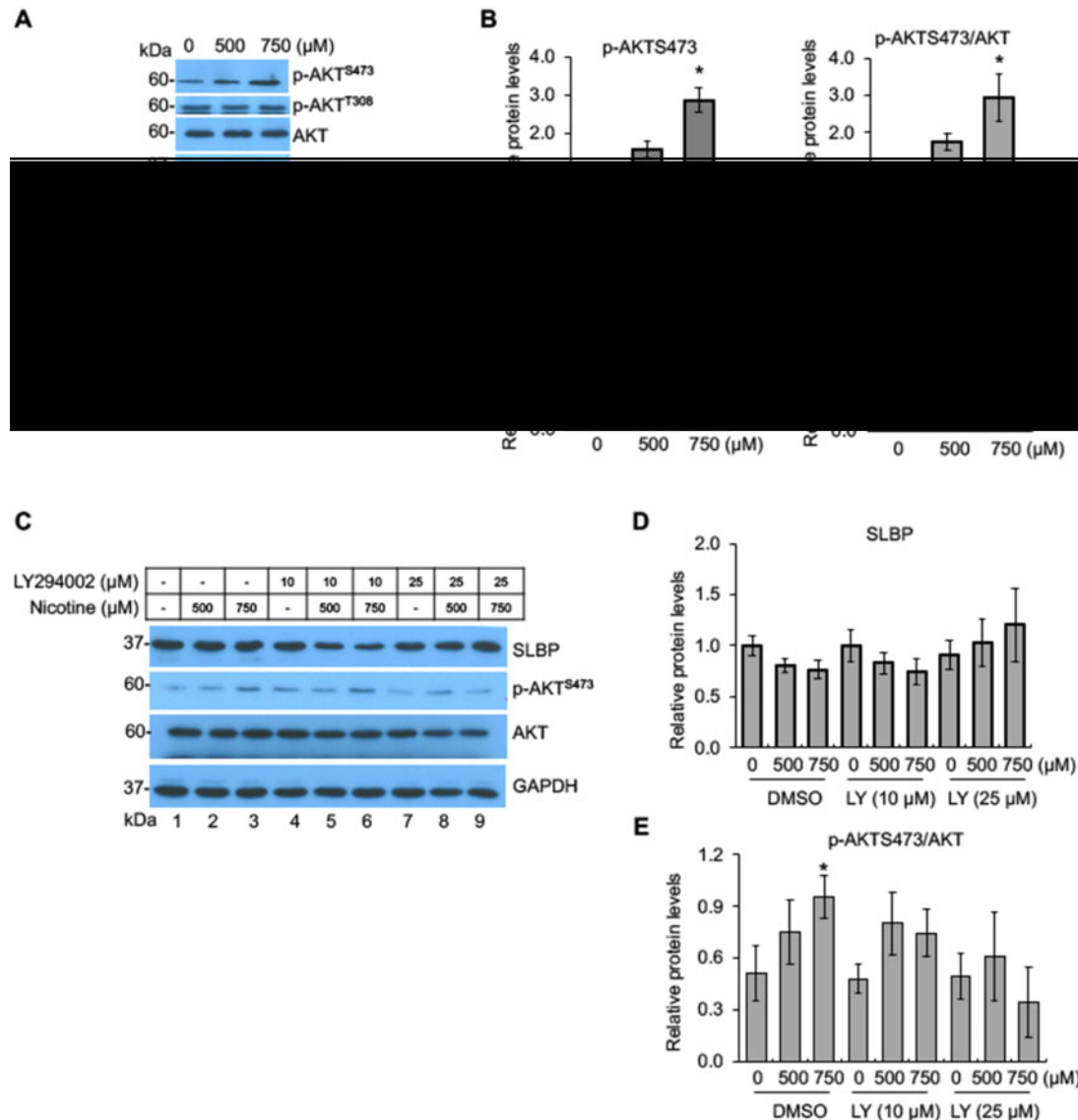


Figure 3. Activation of PI3K/AKT signal transduction pathway by nicotine exposure. A and B, Phosphorylation of AKT at S473 by nicotine. BEAS-2B cells were treated with or without nicotine for 24 h followed by Western blot analysis with indicated antibodies (A). The band intensities were quantified and presented as bar graphs (B). GAPDH was used as an internal control. C–E, Inhibition of PI3K/AKT pathway attenuates nicotine-induced downregulation of SLBP. BEAS-2B cells were treated with or without nicotine for 24 h in the presence or absence of LY294002, an inhibitor of PI3K, and subjected to Western blot with indicated antibodies (C). The band intensities were quantified and presented as bar graphs to show relative quantifications of SLBP (D) and p-AKT^{S473}/AKT (E). GAPDH was used as an internal control. Untreated controls in lane 1 were used as references, which were set to 1. The data shown are the mean \pm SD ($n = 3$). * $p < .05$ versus untreated control group.

(Figs. 5G and I). Together, these results suggest that the $\alpha 1$ catalytic subunit but not the $\alpha 2$ subunit of CK2 is necessary for nicotine-induced SLBP depletion.

The Role of $\alpha 7$ -nAChR in Nicotine-Induced Regulation of CDK1/2, CK2, and AKT

We demonstrated that nicotine exposure activates CDK1/2, CK2, and AKT, which are required for nicotine-induced downregulation of SLBP. To determine if these changes induced by nicotine are $\alpha 7$ -nAChR dependent, we performed Western blot analysis with the cells transfected with the $\alpha 7$ -nAChR siRNA or the control siRNA. In the control cells, $\alpha 7$ -nAChR protein level was increased by about 2-fold following nicotine treatment, whereas no increase was observed in the cells transfected with siRNA for $\alpha 7$ -nAChR, indicating that induction of $\alpha 7$ -nAChR was

successfully inhibited by the $\alpha 7$ -nAChR-specific siRNA (Figs. 6A and B). The levels of p-AKT^{S473}, CDK1, and CK2, but not CDK2 ($p = .056$), were significantly increased following nicotine treatment in the BEAS-2B cells transfected with control siRNA cells, best revealed with 750 μ M nicotine (lanes 1–3 in Figs. 6A and C–F). Importantly, the increases in p-AKT^{S473} and CDK1 and CK2 protein levels mediated by nicotine exposure were prevented by the knockdown of $\alpha 7$ -nAChR (lanes 4–6 in Figs. 6A, C, D, and F). These data suggest that nicotine-induced phosphorylation of AKT at S473 and upregulation of CDK1 and CK2 are $\alpha 7$ -nAChR-dependent.

Nicotine-Induced Cell Transformation Is $\alpha 7$ -nAChR Dependent

To explore a potential role for $\alpha 7$ -nAChR in nicotine-induced cell transformation, we carried out a series of soft agar assays,

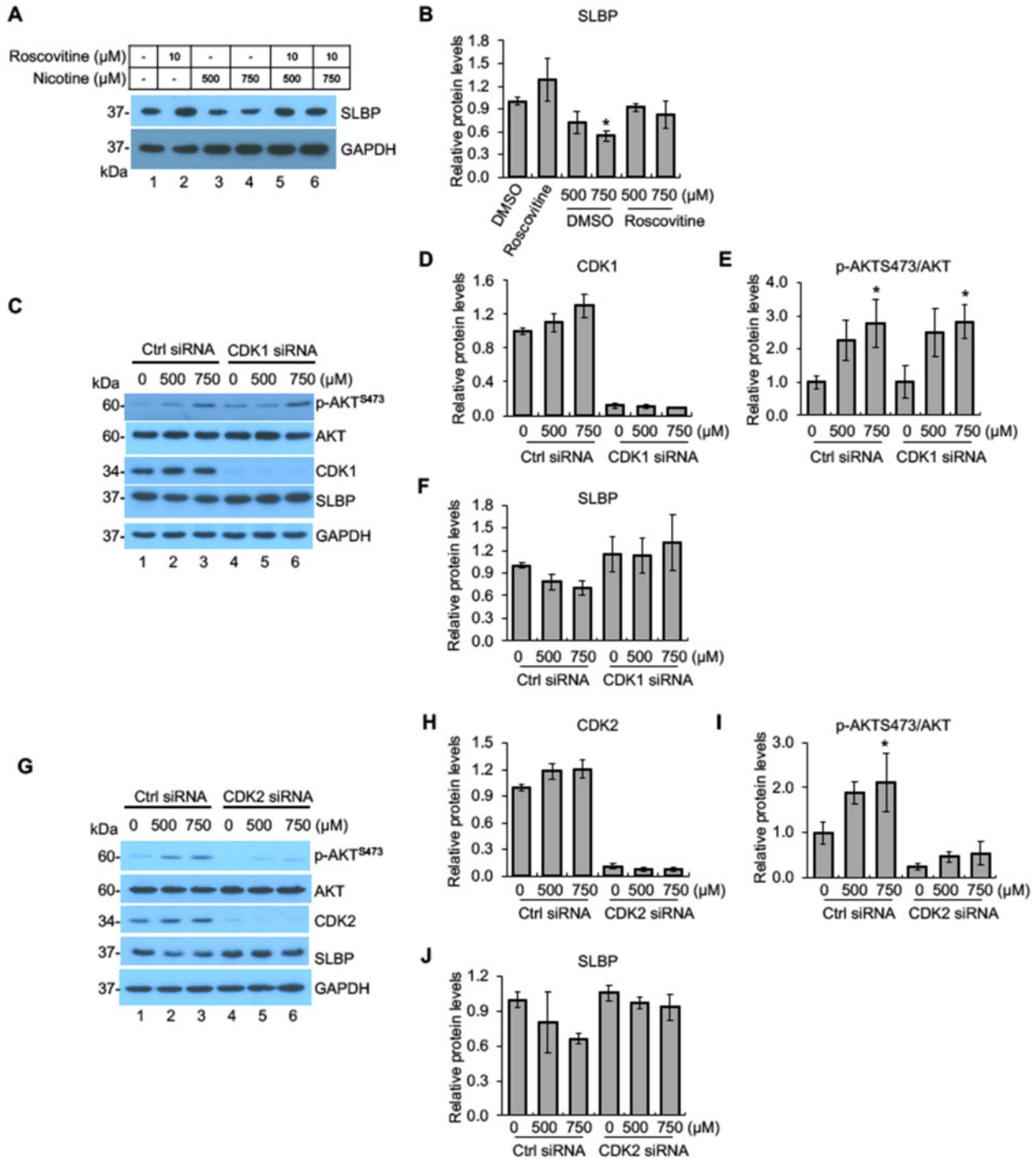


Figure 4. Regulation of nicotine-induced SLBP depletion by CDK1/2. **A** and **B**, Inhibition of CDKs attenuates nicotine-induced downregulation of SLBP. BEAS-2B cells were treated with or without nicotine for 24 h in the presence or absence of roscovitine, an CDK inhibitor, and subjected to Western blot (**A**). The band intensities were quantified and presented as bar graphs to show relative quantifications of SLBP (**B**). GAPDH was used as an internal control. **C–F**, Knockdown of CDK1 by siRNA attenuates nicotine-induced downregulation of SLBP but not phosphorylation of AKT at S473. BEAS-2B cells were transiently transfected with control siRNA or CDK1 siRNA and then treated with or without nicotine for 24 h followed by Western blot analysis with indicated antibodies (**C**). The band intensities were quantified and presented as bar graphs to show relative quantifications of CDK1 (**D**), p-AKTS473/AKT (**E**), and SLBP (**F**). **G–J**, Knockdown of CDK2 by siRNA attenuates nicotine-induced downregulation of SLBP and phosphorylation of AKT at S473. BEAS-2B cells were transiently transfected with control siRNA or CDK2 siRNA and then treated with or without nicotine for 24 h followed by Western blot analysis with indicated antibodies (**G**). The band intensities were quantified and presented as bar graphs to show relative quantifications of CDK2 (**H**), p-AKTS473/AKT (**I**), and SLBP (**J**). Untreated controls in lane 1 were used as references, which were set to 1. The data shown are the mean \pm SD ($n = 3$). * $p < .05$ versus untreated control group.

which measure the ability of cells to grow anchorage independently. We first examined if nicotine can induce cell transformation. Treatment of BEAS-2B cells with 750 μM of nicotine for

24 h facilitated colony formation in soft agar as compared with the untreated control cells (**Figure 7A**). We also examined if “long-term” low-dose nicotine treatment could induce

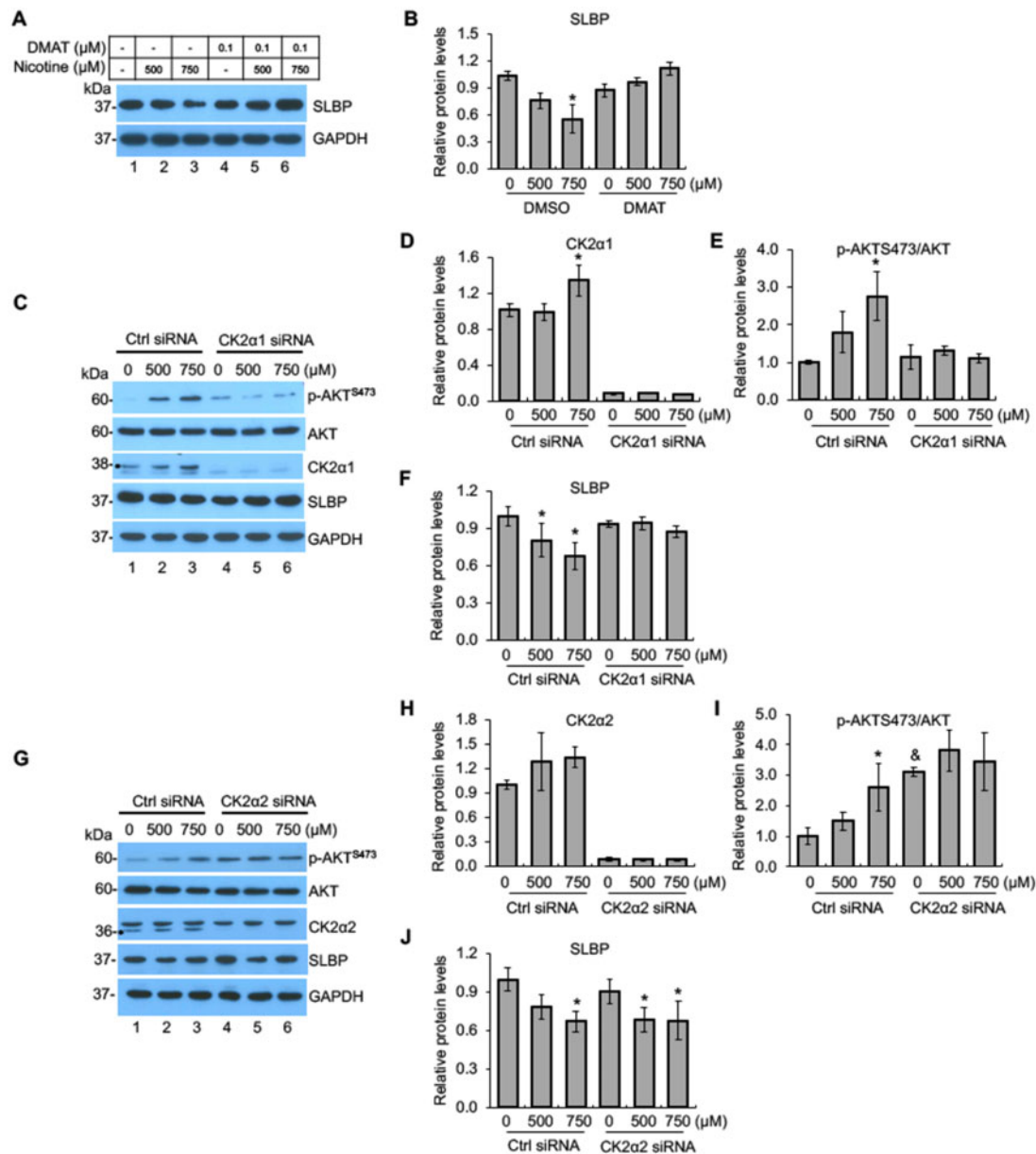


Figure 5. Nicotine-induced downregulation of SLBP is regulated by CK2. A and B, Inhibition of CK2 attenuates nicotine-induced downregulation of SLBP. BEAS-2B cells were treated with or without nicotine for 24 h in the presence or absence of DMAT, an CK2 inhibitor, and subjected to Western blot (A). The band intensities were quantified and presented as bar graphs to show relative quantifications of SLBP (B). GAPDH was used as an internal control. C–F, Knockdown of CK2 α 1 by siRNA attenuates nicotine-induced downregulation of SLBP and phosphorylation of AKT at S473. BEAS-2B cells were transiently transfected with control siRNA or CK2 α 1 siRNA and then treated with or without nicotine for 24 h followed by Western blot analysis with indicated antibodies (C). The band intensities were quantified and presented as bar graphs to show relative quantifications of CK2 α 1 (D), p-AKTS473/AKT (E), and SLBP (F). GAPDH was used as an internal control. G–J, Knockdown of CK2 α 2 by siRNA has no effects on nicotine-induced downregulation of SLBP. BEAS-2B cells were transiently transfected with control siRNA or CK2 α 2 siRNA and then treated with or without nicotine for 24 h followed by Western blot analysis with indicated antibodies (G). The band intensities were quantified and presented as bar graphs to show relative quantifications of CK2 α 2 (H), p-AKTS473/AKT (I), and SLBP (J). GAPDH was used as an internal control. Untreated controls in lane 1 were used as references, which were set to 1. The data shown are the mean \pm SD ($n = 3$). * $p < .05$ versus untreated control group; $^{\#}p < .05$ versus control group in Ctrl siRNA cells in panel K.

anchorage-independent growth of BEAS-2B cells. The cells were treated with 10, 25, and 50 μM of nicotine for 1–4 weeks. Exposure of BEAS-2B cells with 50 μM nicotine for 4 weeks enhanced colony formation in soft agar by about 70% as compared with the 0 μM nicotine treatment group albeit not significantly ($p = .086$) (Figure 7B and Supplementary Figure 4). These results indicate that nicotine is able to induce cell transformation *in vitro* at least under certain conditions.

We then treated BEAS-2B cells with α -BTX, an inhibitor of α 7-nAChR, or transfected the cells with siRNA for α 7-nAChR, prior to exposure of the cells to nicotine, and then performed soft-agar assays. Nicotine-mediated colony formation in soft agar was suppressed by pretreatment of the cells with α -BTX (Figure 7C). Moreover, knockdown of α 7-nAChR by siRNA abolished colony formation in soft agar, regardless of whether the cells were treated with or without nicotine (Figure 7D),

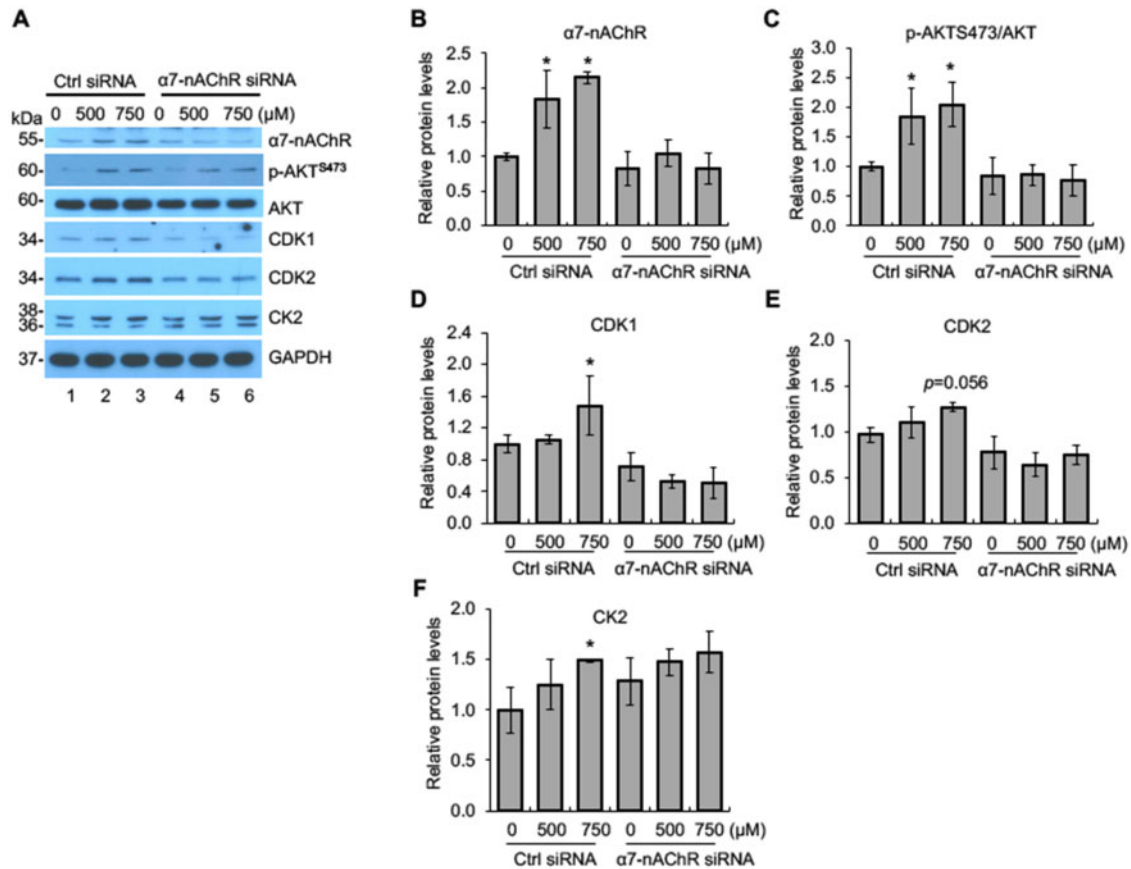


Figure 6. Nicotine-induced activation of AKT, CDK1, and CK2 is $\alpha 7$ -nAChR dependent. A, Knockdown of $\alpha 7$ -nAChR by siRNA attenuates nicotine-induced activation of AKT, CDK1, and CK2. BEAS-2B cells were transiently transfected with control siRNA or $\alpha 7$ -nAChR siRNA and then treated with or without nicotine for 24 h followed by Western blot analysis with indicated antibodies. B–F, The band intensities from (A) were quantified and presented as bar graphs to show relative quantifications of $\alpha 7$ -nAChR (B), p-AKTS473/AKT (C), CDK1 (D), CDK2 (E), and CK2 (F). GAPDH was used as an internal control. The controls in lane 1 were used as references. The data shown are the mean \pm SD ($n = 3$). * $p < .05$ versus control group.

suggesting that $\alpha 7$ -nAChR is required for anchorage-independent cell growth. Taken together, we conclude that nicotine induces cell transformation through the $\alpha 7$ -nAChR.

SLBP Overexpression Inhibits Nicotine-Induced Cell Transformation

Nicotine exposure induced cell transformation via $\alpha 7$ -nAChR. Because nicotine exposure led to SLBP protein reduction and H3 protein upregulation via $\alpha 7$ -nAChR, we explored the role of SLBP depletion in nicotine-induced cell transformation. To this end, we established BEAS-2B cell lines that stably express FLAG-tagged SLBP. We chose 2 SLBP-overexpressing cell clones (SLBP clone 1 and clone 2) that expressed relatively low level of exogenous SLBP (Supplementary Figure 5A) to determine how the overexpression of SLBP affects nicotine-induced cell transformation.

BEAS-2B cells and SLBP clone 1 and clone 2 were treated with either 0, 500, or 750 μ M nicotine for 24 h. In parental BEAS-2B cells, nicotine downregulated SLBP and upregulated polyadenylated H3.1 mRNA and H3 protein (Supplementary Figs. 5A–E). In contrast, overexpression of SLBP in both SLBP clone 1 and 2 prevented nicotine-induced loss of SLBP and increase of polyadenylated H3.1 mRNA and H3 protein (Supplementary Figs. 5A–E). Importantly, although colony numbers in soft agars were increased with statistical significance by treatment of the parental cells with 750 μ M nicotine for 24 h, cells that expressed FLAG-SLBP exhibited no colony formation in soft agar in the presence

or absence of nicotine treatment (Figure 7E). Similar results were obtained when the cells were treated with 50 μ M nicotine for 4 weeks (Figure 7F). These results suggest that SLBP has an inhibitory effect on anchorage-independent cell growth and is likely required for nicotine-induced cell transformation.

Exposure to Nicotine Aerosols Generated from e-Cigs Downregulates SLBP in Normal Human Bronchial Epithelial Primary Cells and in Mice

We used liquid nicotine to demonstrate downregulation of SLBP and subsequent increase in polyadenylated histone H3.1 mRNA and H3 protein level in BEAS-2B cells. It is important to confirm the results with nicotine aerosols generated by e-cigs. The nicotine concentration of e-cig varies between 3 and 36 mg/ml with recent generations of e-cigs containing up to 60 mg/ml of nicotine (Kesimer, 2019). Thus, we generated e-cig aerosols from unflavored e-liquid, which contains 0 or 18 mg/ml nicotine with 50% PG and 50% VG (50:50 PG/VG). FA was used as the control. Exposure of BEAS-2B cells to e-cig aerosols generated from e-liquid with 18 mg/ml nicotine, but not with 0 mg/ml nicotine, dramatically reduced the protein and mRNA levels for SLBP as compared with the FA control group (Figs. 8A, B, and D). Exposure to e-cig aerosols with 18 mg/ml nicotine significantly increased the protein level of H3 (Figs. 8A and C) and polyadenylated H3.1 mRNA as compared with the FA control (Figure 8E). By contrast, exposure to e-cig aerosols without nicotine had no

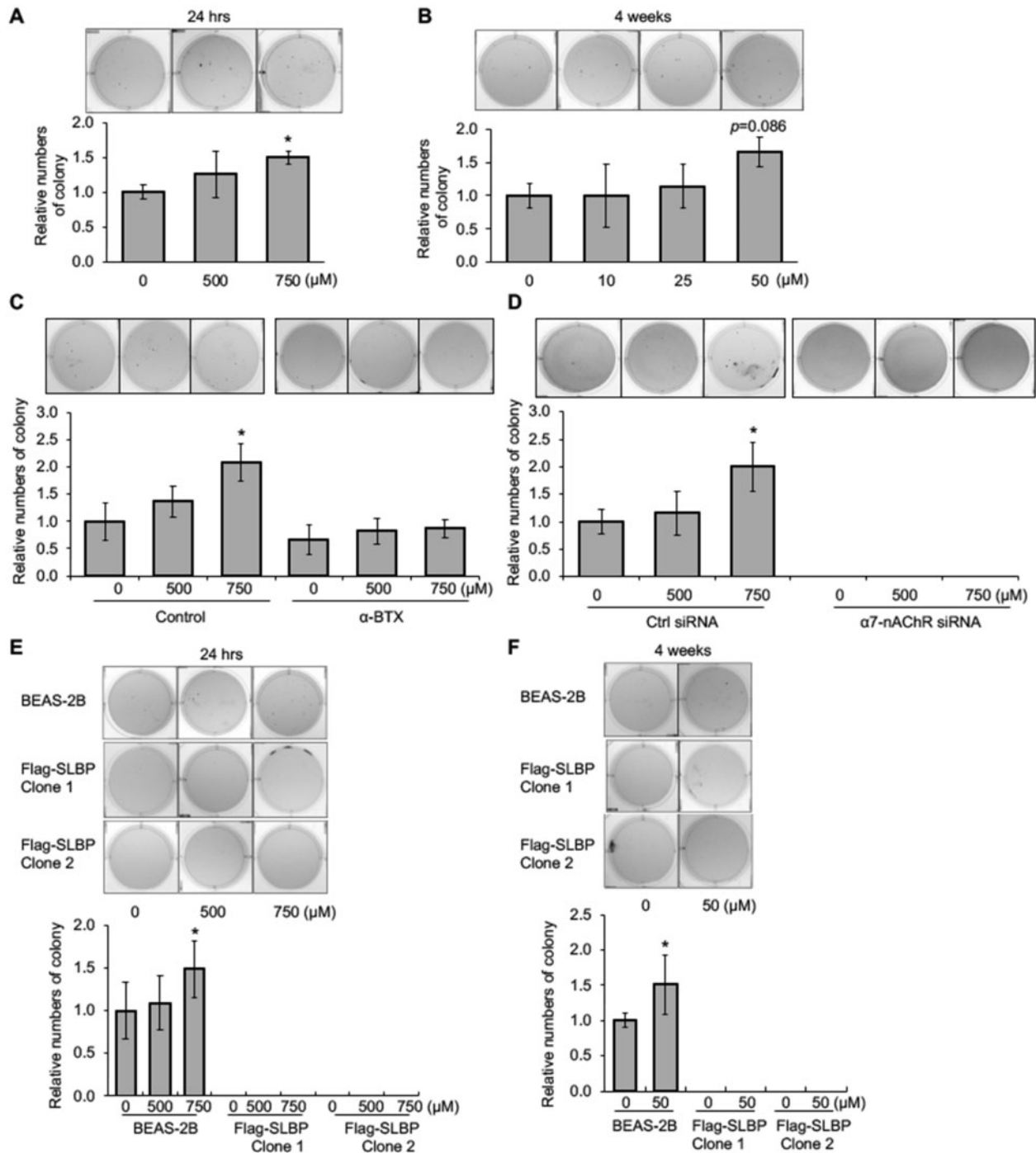


Figure 7. Nicotine induces anchorage-independent cell growth through the $\alpha 7$ -nAChR and overexpression of SLBP rescues nicotine-induced cell transformation. A and B, Exposure of BEAS-2B cells to 750 μ M nicotine for 24 h (A) or 50 μ M for 4 weeks (B) enhances anchorage-independent cell growth. After nicotine treatment, the cells were plated in soft agar, and cultured for 6 weeks. C, Inhibition of $\alpha 7$ -nAChR attenuates nicotine-induced anchorage-independent cell growth. BEAS-2B cells were treated with or without nicotine for 24 h in the presence or absence of α -BTX, an inhibitor of $\alpha 7$ -nAChR, and then subjected to soft agar assays. The cells were grown in soft agar for 6 weeks. D, Knockdown of $\alpha 7$ -nAChR inhibits anchorage-independent cell growth. BEAS-2B cells were transiently transfected with control siRNA or siRNA specific for $\alpha 7$ -nAChR, treated with or without nicotine for 24 h, and then subjected to soft agar assays. The cells were grown in soft agar for 6 weeks. E and F, Soft agar assays. BEAS-2B cells as well as SLBP-overexpressing cells were treated either with 0, 500, and 750 μ M nicotine for 24 h, or with 0 and 50 μ M nicotine for 4 weeks, and then plated in soft agar, cultured for 6 weeks. The data shown are the mean \pm SD ($n = 3$). * $p < .05$ versus control group.

effect on the levels of polyadenylated H3.1 mRNA and H3 protein (Figs. 8A, C, and E). These data indicate that the loss of SLBP and gain of polyadenylated H3.1 mRNA can be induced not only by exposure to liquid nicotine, but also by nicotine aerosols generated by heating e-cig containing nicotine.

Next, we used NHBE cells to validate our data in primary human lung cells. Because the cells grow very slowly with limited passage numbers, we were only able to collect samples for RT-qPCR assays. The level of SLBP mRNA was reduced by exposure of NHBE cells to e-cig aerosols with nicotine, but not by e-cig

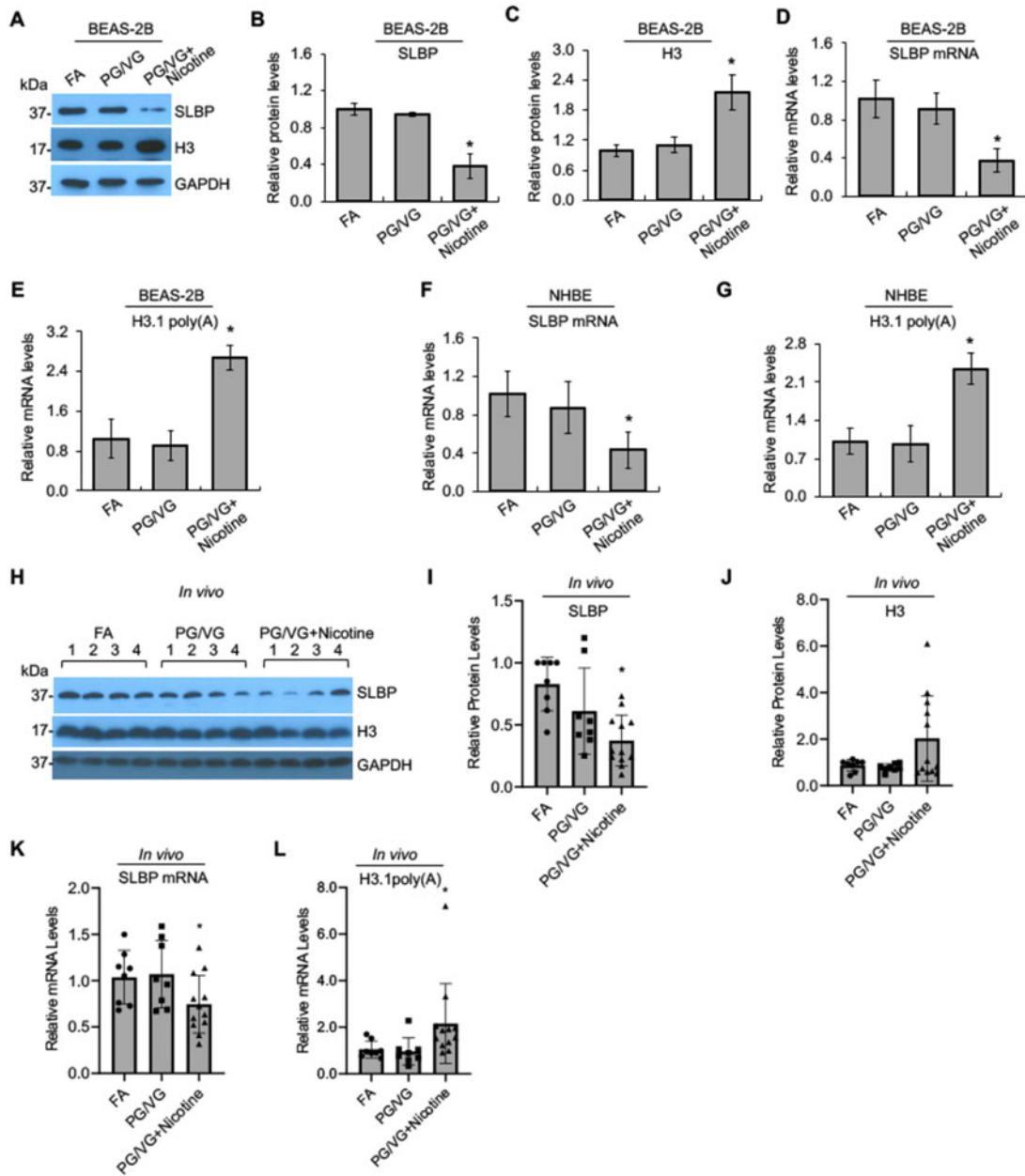


Figure 8. Downregulation of SLBP and polyadenylation of H3.1 mRNA by e-cig aerosols with nicotine in human lung primary cells and in mice. A–C, Western blot detects changes in SLBP and H3 protein levels induced by e-cig aerosols in BEAS-2B cells. BEAS-2B cells were exposed to filtered clean air (FA), e-cig aerosols containing PG/VG and 0 mg/ml nicotine (PG/VG), or e-cig aerosols containing PG/VG and 18 mg/ml nicotine (PG/VG+Nicotine) followed by Western blot analysis. The band intensities were quantified using ImageJ software and presented as bar graphs to show relative quantifications of SLBP (B) and total H3 (C). GAPDH was used as an internal control. The FA control group were used as references. The data shown are the mean \pm SD ($n = 3$). * $p < .05$ versus FA group. D and E: RT-qPCR detects changes in SLBP mRNA and polyadenylated H3.1 mRNA levels induced by e-cig aerosols in BEAS-2B cells. The amount of polyadenylated H3.1 mRNA was measured by RT-qPCR using cDNAs synthesized with oligo (dT) primers. mRNA levels for SLBP and H3.1 were normalized to GAPDH. The data shown are the mean \pm SD ($n = 3$). * $p < .05$ versus FA group. F and G, Changes in SLBP mRNA and polyadenylated H3.1 mRNA levels induced by e-cig aerosols in NHBE primary cells. mRNA levels for SLBP and polyadenylated H3.1 were normalized to GAPDH. The data shown are the mean \pm SD ($n = 3$). * $p < .05$ versus FA group. H–L, Western blot detects changes in SLBP and H3 levels in lung tissues of mice exposed to e-cig aerosols. H–J) female mice were exposed FA, PG/VG, or PG/VG plus 36 mg/ml of nicotine 5 days a week for 3 months. Lung tissues were collected and protein and mRNA levels were analyzed by Western blot (H–J) or RT-qPCR (K, L), respectively. GAPDH was used as an internal control. The data are shown for each individual mouse. Relative protein levels were calculated based on band intensity. Error bars represent SD ($n = 8$ for FA and PG/VG groups; $n = 12$ for nicotine exposure group). * $p < .05$ versus FA group.

aerosols without nicotine as compared with the FA control (Figure 8F). Furthermore, exposure of the primary human lung cells to nicotine aerosols increased the level of polyadenylated H3.1 mRNA by more than 2-fold (Figure 8G). These data confirm the impact of nicotine on SLBP expression and polyadenylation of H3.1 mRNA in human lung primary epithelial cells.

Changes in SLBP expression and polyadenylation of H3.1 mRNA were also measured in lung tissues collected from female A/J mice exposed to FA, e-cigs without nicotine (PG/VG group), or e-cigs with 36 mg/ml of nicotine (PG/VG plus nicotine group). The mice were exposed 5 days a week for 3 months and analyzed 2.5 months later. Western blot and RT-qPCR results

showed that both protein and mRNA levels of SLBP were decreased in the nicotine exposure group, but not in the PG/VG group, with statistical significance ($p < .05$) as compared with the FA control group (Figs. 8H, I, and K). Moreover, the level of polyadenylated H3.1 mRNA was also increased in lung tissues of mice exposed to e-cig aerosols with nicotine (nicotine group), but not to e-cig without nicotine (PG/VG group) (Figure 8L). The total H3 protein levels appeared to be increased in the nicotine group, but not in the PG/VG group as compared with the FA control, however, this did not reach statistical difference (Figs. 8H and J). These results suggest that nicotine exposure downregulates SLBP levels and induces polyadenylation of canonical histone mRNA *in vivo*.

DISCUSSION

In the present study, using immortalized NHBE BEAS-2B cells, human primary NHBE cells, and an *in vivo* exposure, we demonstrate that nicotine exposure induces the loss of SLBP and the gain of polyadenylated canonical histone H3.1 mRNA. Treatment of BEAS-2B cells with liquid nicotine resulted in a decrease in both protein and mRNA levels of SLBP and the increase in the levels of H3.1 mRNA with poly(A) tail. Importantly, the same results were obtained with e-cig aerosols, which were generated by heating e-cig liquid containing nicotine. The results were not likely due to other components in the e-cig liquid, such as PG/VG, because the aerosols from e-cig without nicotine did not change the levels of SLBP and polyadenylated H3.1 mRNA as compared with the FA control. Moreover, the results were not likely BEAS-2B cells- and immortalized cells-specific, because exposure of the primary NHBE cells to nicotine aerosols also downregulated SLBP mRNA levels and increased the levels of polyadenylated H3.1 mRNA. These changes were seen in animal exposure studies as well. Mice exposed to the aerosols from e-cig with nicotine, but not from e-cig without nicotine, exhibited lower levels of SLBP protein and mRNA levels as well as higher levels of polyadenylated H3.1 mRNA in the lung tissues as compared with the FA control groups. Taking together, we conclude that nicotine exposure induces the SLBP depletion and polyadenylation of canonical H3.1 mRNA.

The loss of SLBP is associated with genomic instability (Kodama *et al.*, 2002; Salzler *et al.*, 2009). Although SLBP is involved in the most processes of biosynthesis of canonical histones, including their pre-mRNA processing, mRNA stability, nuclear export, and translation. Aberrant 3' processing, ie, polyadenylation of canonical histone mRNAs appeared to be the major mechanism for SLBP-associated genomic instability, because overexpression of polyadenylated H3.1 mRNA led to deregulation of cancer-associated genes, including lung-cancer related genes, aberrant cell cycle progress as well as chromosome aneuploidy and aberrations (Chen *et al.*, 2020). Not surprisingly, both knockdown of SLBP and polyadenylation of H3.1 mRNA were able to enhance anchorage-independent growth of BEAS-2B cells, indicating a critical role for the loss of SLBP and subsequent acquisition of a poly(A) tail at the 3' end of H3.1 mRNA in cell transformation (Chen *et al.*, 2020). This current study showed that although nicotine exposure decreased the level of SLBP, overexpression of SLBP was able to prevent the nicotine-induced cell transformation. This effect was likely attributable to reduced induction of polyadenylated H3.1 mRNA, because overexpression of SLBP attenuated nicotine-induced polyadenylation of canonical histone mRNAs. We propose that the loss of SLBP and the gain of polyadenylated canonical

histone mRNAs, in particular H3.1 mRNA, may represent a novel mechanism for nicotine toxicity and cell transformation.

Nicotine acts primarily by activating nAChRs, which are expressed not only in neuronal cells, but also in nonneuronal epithelial and endothelial cells (Cattaneo *et al.*, 1993; Cheng *et al.*, 2020). Deregulation of the nAChRs is often observed in many cancers, including lung cancer (Mucchietto *et al.*, 2016; Schaal and Chellappan, 2014). In our study, immunofluorescence staining revealed upregulation of $\alpha 7$ -nAChR following nicotine treatment. $\alpha 7$ -nAChR was required for nicotine-induced SLBP downregulation because an inhibitor of $\alpha 7$ -nAChR, but not of $\alpha 3/\alpha 4$ -nAChRs, attenuated nicotine-induced loss of SLBP. This was further supported by the observation that the SLBP level was not changed by nicotine exposure in the $\alpha 7$ -nAChR knockdown cells by siRNA. Our study further demonstrated that activation of $\alpha 7$ -nAChR and subsequent depletion of SLBP are required for nicotine-mediated cell transformation. Tang *et al.* reported that nicotine causes lung carcinogenesis in mice through inducing DNA damage and inhibiting DNA repair (Tang *et al.*, 2019). Our data suggested that non-genotoxic function of nicotine, ie, activation of $\alpha 7$ -nAChR and subsequent downregulation of SLBP and polyadenylation of canonical histone mRNAs, might be another cause or significant contributor to the nicotine-induced carcinogenesis. Another implication of this study is that even without diffusion to the cells, nicotine may play an important role in nicotine-induced toxicity/carcinogenicity via binding to and activating certain receptors on cell membrane.

Previous studies have demonstrated that activation of nAChRs can trigger a varieties of downstream signal pathways, including PI3K/AKT pathway. Our data showed that nicotine induced phosphorylation of AKT at S473 but not at T308. This was different from the previous results by West *et al.* where they showed that both S473 and T308 of AKT were phosphorylated by nicotine treatment (West *et al.*, 2003). Differences in the cell types and thus the composition of nAChR subunits, and doses and durations of nicotine exposures were likely attributable to the observed differences between 2 studies. Moreover, the phosphorylation of AKT at T308 appeared to be a transient change with peak levels at 15–30 min post treatment (West *et al.*, 2003), which might be another reason why we did not see the change as we measured the phosphorylation status of AKT after 24 h of treatment. Although it is not clear from the current study if nicotine-induced activation of PI3K/AKT pathway is required for downregulation of SLBP, it is possible that AKT may downregulate the SLBP level both by transcriptional deregulation and by proteasome-mediated protein degradation process given that AKT can target numerous functional protein classes including transcription factors and E3-ubiquitin ligases among many others.

In normal cells, the SLBP levels are mainly regulated by a posttranslational mechanism. Phosphorylation of SLBP at T61 by cyclin A/CDK1 and T60 by CK2 are critical for degradation of SLBP by the SCF (SKP1-CUL1-F-box protein) ubiquitin ligase complex (Dankert *et al.*, 2016). Roscovitine, an inhibitor of CDKs including CDK1 and CDK2, was able to rescue nicotine-induced downregulation of SLBP protein level. In addition, the SLBP loss induced by nicotine was reversed either by CDK1 knockdown or by CDK2 knockdown, suggesting that both CDK1 and CDK2 might play roles in nicotine-induced SLBP downregulation. However, further research is needed in the future to confirm this possibility given that nicotine-induced SLBP loss was not statistically significant in the control siRNA cells (Figure 4). Interestingly, nicotine-induced p-AKT^{S473} was not changed by

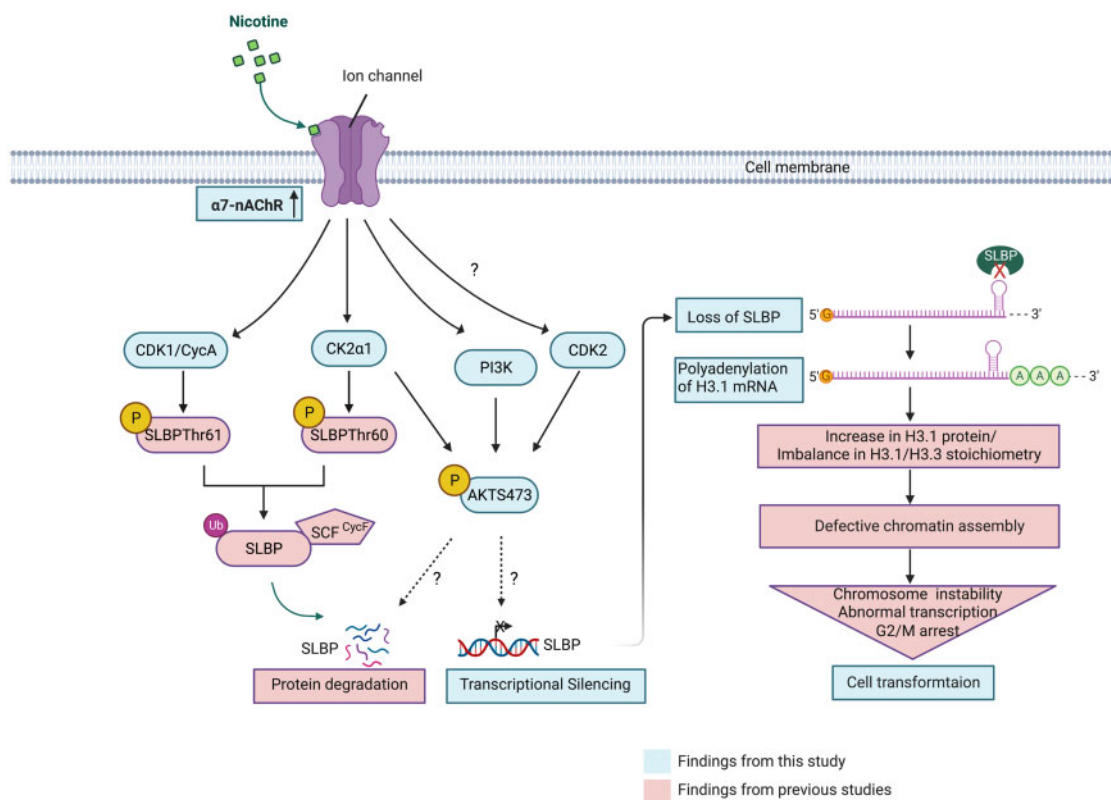


Figure 9. Schematic summary of possible mechanism of nicotine-induced downregulation of SLBP and cell transformation. The graphic was created with BioRender.com.

CDK1 knockdown but was prevented by CDK2 knockdown. These results indicate that CDK1 might downregulate SLBP expression. AKT is independently probably through direct phosphorylation of SLBP, whereas CDK2 might be involved in SLBP downregulation through activating AKT. It is known that CDK2/cyclin A2 phosphorylates AKT at both S477 and T479, triggering the canonical AKT-pS473 phosphorylation to promote AKT activation in response to several upstream signals (Liu *et al.*, 2014).

It has been known that the phosphorylation of SLBP by the tumorigenic potential protein kinase CK2 is primed by the phosphorylation by cyclin A/CDK1, both are required for SLBP degradation (Koseoglu *et al.*, 2008). We demonstrate here that nicotine-induced downregulation of SLBP requires activation of CK2 α 1 catalytic subunit. Nicotine-induced phosphorylation of AKT at S473 was attenuated by the CK2 α 1 knockdown, indicating that CK2 is required for nicotine-induced activation of PI3K/AKT pathway. Moreover, it is known that CK2 can indirectly regulate AKT activity. For example, CK2 inhibits PTEN phosphatase activity, causing AKT activity; CK2 phosphorylation of mTOR kinases enhanced the AKT upstream activator mTORC2, which is responsible for S473 phosphorylation of AKT (Alcaraz *et al.*, 2020). Thus, in addition to direct phosphorylation of SLBP by CK2 and subsequent degradation, activation of AKT pathway by CK2 might also be involved in the nicotine-induced SLBP depletion.

α 7-nAChR was required for nicotine-induced activation of CDK1, CK2, and PI3K/AKT pathway. Our findings lend support to the importance of nAChR in nicotine toxicity and potential carcinogenicity, because both inhibition of α 7-nAChR by an inhibitor or by siRNA knockdown reversed nicotine-induced cell transformation. As PI3K/AKT pathway and kinases like CDK1/2 and CK2 possess many downstream effectors, it is likely that nicotine

may exert its effects not only through targeting SLBP but also other effectors. We propose that nicotine causes SLBP depletion and polyadenylation of canonical histone mRNAs through activation of α 7-nAChR and a series of downstream signal transduction pathways, involving PI3K/AKT, CDK1/2, and CK2 (Figure 9). This mechanism may be critical for nicotine-induced bronchial epithelial cell transformation and carcinogenesis.

A key question needs to be addressed among many others is how PI3K/AKT, CDK1/2, and CK2 are activated by nicotine exposure. Previous studies have demonstrated that nAChR can activate different kinases in a Ca^{2+} -dependent or Ca^{2+} -independent manner. Activation of nAChR induces influx of Ca^{2+} , resulting in increased intracellular Ca^{2+} concentration, which triggers binding of Ca^{2+} to CaM (calmodulin), a major Ca^{2+} sensor. Ca^{2+} /CaM then interacts with the family of CaM kinases (CaMKs) and activates them by releasing their catalytic domain from autoinhibitory domain. A number of studies have shown that α 7-nAChR-mediated activation of MAPK and PI3K pathways requires Ca^{2+} -dependent CaMKII activation (Chernyavsky *et al.*, 2009, 2010; Gubbins *et al.*, 2010). Moreover, α 7-nAChR can mediate activation of MAPK and PI3K pathways Ca^{2+} independently through activation of Jak2 or FYN tyrosine kinases (Chernyavsky *et al.*, 2009, 2010; de Jonge *et al.*, 2005; Kihara *et al.*, 2001). The mechanisms that control nicotine-induced activation of PI3K/AKT, CDK1/2, and CK2, Ca^{2+} dependent or independent, and their interplays need further investigation in the future.

SUPPLEMENTARY DATA

Supplementary data are available at Toxicological Sciences online.

ACKNOWLEDGMENTS

We thank John Adragna and Terry Gorden for their assistance in cell exposure to e-cig aerosols.

AUTHOR CONTRIBUTIONS

C.J. conceived the study; Q.S. and C.J. designed the experiments; Q.S. and D.C. performed most of the experiments and data analysis; A.R. conducted animal exposure under supervision of J.Z. and G.G.; G.G., Q.S., and D.C. collected mouse lung tissues; Q.S. and C.J. wrote the manuscript with input from other coauthors.

FUNDING

Foundation for the U.S. National Institutes of Health (R01ES029359, R01ES030583 to C.J.).

DECLARATION OF CONFLICTING INTERESTS

The authors declared no potential conflicts of interest with respect to the research, authorship, and/or publication of this article.

REFERENCES

- Albuquerque, E. X., Pereira, E. F., Alkondon, M., and Rogers, S. W. (2009). Mammalian nicotinic acetylcholine receptors: From structure to function. *Physiol. Rev.* **89**, 73–120.
- Alcaraz, E., Vilardell, J., Borgo, C., Sarro, E., Plana, M., Marin, O., Pinna, L. A., Bayascas, J. R., Meseguer, A., Salvi, M., et al. (2020). Effects of CK2beta subunit down-regulation on Akt signalling in HK-2 renal cells. *PLoS One* **15**, e0227340.
- Armitage, A. K., Dollery, C. T., George, C. F., Houseman, T. H., Lewis, P. J., and Turner, D. M. (1975). Absorption and metabolism of nicotine from cigarettes. *Br. Med. J.* **4**, 313–316.
- Bold, K. W., Kong, G., Morean, M., Gueorguieva, R., Camenga, D. R., Simon, P., Davis, D. R., Jackson, A., and Krishnan-Sarin, S. (2021). Trends in various e-cigarette devices used by high school adolescents from 2017–2019. *Drug Alcohol Depend.* **219**, 108497.
- Bradford, B. R., and Jin, C. (2021). Stem-loop binding protein and metal carcinogenesis. *Semin. Cancer Biol.* **76**, 38–44.
- Brocato, J., Chen, D., Liu, J., Fang, L., Jin, C., and Costa, M. (2015). A potential new mechanism of arsenic carcinogenesis: Depletion of stem-loop binding protein and increase in polyadenylated canonical histone H3.1 mRNA. *Biol. Trace Elem. Res.* **166**, 72–81.
- Brocato, J., Fang, L., Chervona, Y., Chen, D., Kiok, K., Sun, H., Tseng, H. C., Xu, D., Shamy, M., Jin, C., et al. (2014). Arsenic induces polyadenylation of canonical histone mRNA by down-regulating stem-loop-binding protein gene expression. *J. Biol. Chem.* **289**, 31751–31764.
- Cattaneo, M. G., Codignola, A., Vicentini, L. M., Clementi, F., and Sher, E. (1993). Nicotine stimulates a serotonergic autocrine loop in human small-cell lung carcinoma. *Cancer Res.* **53**, 5566–5568.
- Chen, D., Chen, Q. Y., Wang, Z., Zhu, Y., Kluz, T., Tan, W., Li, J., Wu, F., Fang, L., Zhang, X., et al. (2020). Polyadenylation of histone H3.1 mRNA promotes cell transformation by displacing H3.3 from gene regulatory elements. *iScience* **23**, 101518.
- Cheng, W. L., Chen, K. Y., Lee, K. Y., Feng, P. H., and Wu, S. M. (2020). Nicotinic-nAChR signaling mediates drug resistance in lung cancer. *J. Cancer* **11**, 1125–1140.
- Chernyavsky, A. I., Arredondo, J., Galitovskiy, V., Qian, J., and Grando, S. A. (2010). Upregulation of nuclear factor-kappaB expression by SLURP-1 is mediated by alpha7-nicotinic acetylcholine receptor and involves both ionic events and activation of protein kinases. *Am. J. Physiol. Cell Physiol.* **299**, C903–911.
- Chernyavsky, A. I., Arredondo, J., Qian, J., Galitovskiy, V., and Grando, S. A. (2009). Coupling of ionic events to protein kinase signaling cascades upon activation of alpha7 nicotinic receptor: Cooperative regulation of alpha2-integrin expression and rho kinase activity. *J. Biol. Chem.* **284**, 22140–22148.
- Church, J. S., Chace-Donahue, F., Blum, J. L., Ratner, J. R., Zelikoff, J. T., and Schwartz, J. J. (2020). Neuroinflammatory and behavioral outcomes measured in adult offspring of mice exposed prenatally to e-cigarette aerosols. *Environ. Health Perspect.* **128**, 47006.
- Cicenas, J., Kalyan, K., Sorokinas, A., Stankunas, E., Levy, J., Meskinyte, I., Stankevicius, V., Kaupinis, A., and Valius, M. (2015). Roscovitine in cancer and other diseases. *Ann. Transl. Med.* **3**, 135.
- Dankert, J. F., Rona, G., Clijsters, L., Geter, P., Skaar, J. R., Bermudez-Hernandez, K., Sassani, E., Fenyö, D., Ueberheide, B., Schneider, R., et al. (2016). Cyclin F-mediated degradation of SLBP limits H2a.X accumulation and apoptosis upon genotoxic stress in G2. *Mol. Cell* **64**, 507–519.
- de Jonge, W. J., van der Zanden, E. P., The, F. O., Bijlsma, M. F., van Westerloo, D. J., Bennink, R. J., Berthoud, H. R., Uematsu, S., Akira, S., van den Wijngaard, R. M., et al. (2005). Stimulation of the vagus nerve attenuates macrophage activation by activating the Jak2-STAT3 signaling pathway. *Nat. Immunol.* **6**, 844–851.
- Grando, S. A. (2014). Connections of nicotine to cancer. *Nat. Rev. Cancer* **14**, 419–429.
- Gubbins, E. J., Gopalakrishnan, M., and Li, J. (2010). Alpha7 nAChR-mediated activation of map kinase pathways in PC12 cells. *Brain Res.* **1328**, 1–11.
- Kesimer, M. (2019). Another warning sign: High nicotine content in electronic cigarettes disrupts mucociliary clearance, the essential defense mechanism of the lung. *Am. J. Respir. Crit. Care Med.* **200**, 1082–1084.
- Kihara, T., Shimohama, S., Sawada, H., Honda, K., Nakamizo, T., Shibasaki, H., Kume, T., and Akaike, A. (2001). Alpha 7 nicotinic receptor transduces signals to phosphatidylinositol 3-kinase to block a beta-amyloid-induced neurotoxicity. *J. Biol. Chem.* **276**, 13541–13546.
- Kodama, Y., Rothman, J. H., Sugimoto, A., and Yamamoto, M. (2002). The stem-loop binding protein CDL-1 is required for chromosome condensation, progression of cell death and morphogenesis in *Caenorhabditis elegans*. *Development* **129**, 187–196.
- Koseoglu, M. M., Graves, L. M., and Marzluff, W. F. (2008). Phosphorylation of threonine 61 by cyclin a/Cdk1 triggers degradation of stem-loop binding protein at the end of S phase. *Mol. Cell. Biol.* **28**, 4469–4479.
- Kwon, E., Adams, Z., and Seo, D. C. (2021). Trajectories and determinants of adolescents' nicotine product use risk among U.S. adolescents in a nationally representative sample of longitudinal cohort. *Addict. Behav.* **116**, 106812.
- Lanzotti, D. J., Kaygun, H., Yang, X., Duronio, R. J., and Marzluff, W. F. (2002). Developmental control of histone mRNA and dSLBP synthesis during drosophila embryogenesis and the

- role of dSLBP in histone mRNA 3' end processing in vivo. *Mol. Cell. Biol.* **22**, 2267–2282.
- Lauterstein, D. E., Tijerina, P. B., Corbett, K., Akgol Oksuz, B., Shen, S. S., Gordon, T., Klein, C. B., and Zelikoff, J. T. (2016). Frontal cortex transcriptome analysis of mice exposed to electronic cigarettes during early life stages. *Int. J. Environ. Res. Public Health* **13**, 417.
- Lee, H. W., Park, S. H., Weng, M. W., Wang, H. T., Huang, W. C., Lepor, H., Wu, X. R., Chen, L. C., and Tang, M. S. (2018). E-cigarette smoke damages DNA and reduces repair activity in mouse lung, heart, and bladder as well as in human lung and bladder cells. *Proc. Natl. Acad. Sci. U.S.A.* **115**, E1560–e1569.
- Lindell, G., Farnebo, L. O., Chen, D., Nexø, E., Rask Madsen, J., Bukhave, K., and Graffner, H. (1993). Acute effects of smoking during modified sham feeding in duodenal ulcer patients. An analysis of nicotine, acid secretion, gastrin, catecholamines, epidermal growth factor, prostaglandin E₂, and bile acids. *Scand. J. Gastroenterol.* **28**, 487–494.
- Liu, P., Begley, M., Michowski, W., Inuzuka, H., Ginzberg, M., Gao, D., Tsou, P., Gan, W., Papa, A., Kim, B. M., et al. (2014). Cell-cycle-regulated activation of Akt kinase by phosphorylation at its carboxyl terminus. *Nature* **508**, 541–545.
- Mathijs, K., Brauers, K. J., Jennen, D. G., Lizarraga, D., Kleinjans, J. C., and van Delft, J. H. (2010). Gene expression profiling in primary mouse hepatocytes discriminates true from false-positive genotoxic compounds. *Mutagenesis* **25**, 561–568.
- Mucchietto, V., Crespi, A., Fasoli, F., Clementi, F., and Gotti, C. (2016). Neuronal acetylcholine nicotinic receptors as new targets for lung cancer treatment. *Curr. Pharm. Des.* **22**, 2160–2169.
- Paleari, L., Catassi, A., Ciarlo, M., Cavaliere, Z., Bruzzo, C., Servent, D., Cesario, A., Chessa, L., Cilli, M., Piccardi, F., et al. (2008). Role of alpha7-nicotinic acetylcholine receptor in human non-small cell lung cancer proliferation. *Cell Prolif.* **41**, 936–959.
- Russell, M. A., Jarvis, M., Iyer, R., and Feyerabend, C. (1980). Relation of nicotine yield of cigarettes to blood nicotine concentrations in smokers. *Br. Med. J.* **280**, 972–976.
- Russo, P., Catassi, A., Cesario, A., and Servent, D. (2006). Development of novel therapeutic strategies for lung cancer: Targeting the cholinergic system. *Curr. Med. Chem.* **13**, 3493–3512.
- Saccone, N. L., Culverhouse, R. C., Schwantes-An, T. H., Cannon, D. S., Chen, X., Cichon, S., Giegling, I., Han, S., Han, Y., Keskitalo-Vuokko, K., et al. (2010). Multiple independent loci at chromosome 15q25.1 affect smoking quantity: A meta-analysis and comparison with lung cancer and COPD. *PLoS Genet.* **6**, e1001053.
- Salzler, H. R., Davidson, J. M., Montgomery, N. D., and Duronio, R. J. (2009). Loss of the histone pre-mRNA processing factor stem-loop binding protein in drosophila causes genomic instability and impaired cellular proliferation. *PLoS One* **4**, e8168.
- Schaal, C., and Chellappan, S. P. (2014). Nicotine-mediated cell proliferation and tumor progression in smoking-related cancers. *Mol. Cancer Res.* **12**, 14–23.
- Sullivan, E., Santiago, C., Parker, E. D., Dominski, Z., Yang, X., Lanzotti, D. J., Ingledue, T. C., Marzluff, W. F., and Duronio, R. J. (2001). Drosophila stem loop binding protein coordinates accumulation of mature histone mRNA with cell cycle progression. *Genes Dev.* **15**, 173–187.
- Sullivan, K. D., Steiniger, M., and Marzluff, W. F. (2009). A core complex of CPSF73, CPSF100, and Symplekin may form two different cleavage factors for processing of poly(a) and histone mRNAs. *Mol. Cell.* **34**, 322–332.
- Tang, M. S., Wu, X. R., Lee, H. W., Xia, Y., Deng, F. M., Moreira, A. L., Chen, L. C., Huang, W. C., and Lepor, H. (2019). Electronic-cigarette smoke induces lung adenocarcinoma and bladder urothelial hyperplasia in mice. *Proc. Natl. Acad. Sci. U.S.A.* **116**, 21727–21731.
- van Kesteren, P. C., Zwart, P. E., Pennings, J. L., Gottschalk, W. H., Kleinjans, J. C., van Delft, J. H., van Steeg, H., and Luijten, M. (2011). Deregulation of cancer-related pathways in primary hepatocytes derived from DNA repair-deficient Xpa^{-/-}p53^{+/-} mice upon exposure to benzo[a]pyrene. *Toxicol. Sci.* **123**, 123–132.
- West, K. A., Brognard, J., Clark, A. S., Linnoila, I. R., Yang, X., Swain, S. M., Harris, C., Belinsky, S., and Dennis, P. A. (2003). Rapid Akt activation by nicotine and a tobacco carcinogen modulates the phenotype of normal human airway epithelial cells. *J. Clin. Invest.* **111**, 81–90.
- Whitfield, M. L., Zheng, L. X., Baldwin, A., Ohta, T., Hurt, M. M., and Marzluff, W. F. (2000). Stem-loop binding protein, the protein that binds the 3' end of histone mRNA, is cell cycle regulated by both translational and posttranslational mechanisms. *Mol. Cell. Biol.* **20**, 4188–4198.
- Xiang, T., Fei, R., Wang, Z., Shen, Z., Qian, J., and Chen, W. (2016). Nicotine enhances invasion and metastasis of human colorectal cancer cells through the nicotinic acetylcholine receptor downstream p38 MAPK signaling pathway. *Oncol. Rep.* **35**, 205–210.
- Zelikoff, J. T., Parmalee, N. L., Corbett, K., Gordon, T., Klein, C. B., and Aschner, M. (2018). Microglia activation and gene expression alteration of neurotrophins in the hippocampus following early-life exposure to e-cigarette aerosols in a murine model. *Toxicol. Sci.* **162**, 276–286.
- Zhao, Y. (2016). The oncogenic functions of nicotinic acetylcholine receptors. *J. Oncol.* **2016**, 9650481.